Class. Quantum Grav. **16** (1999) 1889–1916. Printed in the UK PII: S0264-9381(99)98471-X

Stability of gravitational and electromagnetic geons

G P Perry and F I Cooperstock

Department of Physics and Astronomy, University of Victoria, PO Box 3055, Victoria, BC V8W 3P6, Canada

Received 19 October 1998, in final form 4 March 1999

Abstract. Recent work on gravitational geons is extended to examine the stability properties of gravitational and electromagnetic geon constructs. All types of geons must possess the property of regularity, self-consistency and quasi-stability on a time-scale much longer than the period of the comprising waves. Standard perturbation theory, modified to accommodate time-averaged fields, is used to test the requirement of quasi-stability. It is found that the modified perturbation theory results in an internal inconsistency. The time-scale of evolution is found to be of the same order of magnitude as the period of the comprising waves. This contradicts the requirement of slow evolution. Thus not all of the requirements for the existence of electromagnetic or gravitational geons are met though perturbation theory. From this result it cannot be concluded that an electromagnetic or a gravitational geon is a viable entity. The broader implications of the result are discussed with particular reference to the problem of gravitational energy.

PACS number: 0425

1. Introduction

The examination of the basic properties of the gravitational field as compared to other physical fields has concentrated around the recently revived study of gravitational geons. The concept of a structure comprised of electromagnetic waves held together by its own gravitational attraction was first conceived by Wheeler [1]. The extension of this idea using only gravitational waves was first studied by Brill and Hartle [2]. Their approach was to consider a strongly curved static 'background geometry' $\gamma_{\mu\nu}$ on top of which a small ripple $h_{\mu\nu}$ resided, satisfying a linear wave equation. The wave frequency was assumed to be so high as to create a sufficiently large effective energy density, which served as the source of the background $\gamma_{\mu\nu}$, taken to be spherically symmetric on a time average. They claimed to have found a solution with a flat-space spherical interior, a Schwarzschild exterior and a thin-shell separation meant to be created by high-frequency gravitational waves. With the mass M identified from the exterior metric, there would follow an unambiguous realization of the gravitational geon as described above. It has since been shown [3–5] that the Brill and Hartle model does not implement the properties of high-frequency waves, nor can the spacetime be taken as singularity-free.

It was proposed by Cooperstock, Faraoni and Perry [3–5] (henceforth referred to as CFP) that a satisfactory gravitational geon model must be constructed and solved in a manner similar to that of Wheeler's [1] electromagnetic geon model. Such a model necessarily requires firstly that the Einstein field equations be solved in a self-consistent manner while satisfying the regularity conditions. Secondly, it is required that the configuration represented by the metric $\gamma_{\mu\nu}$ be quasi-stable over a time-scale much larger than the typical period of its gravitational wave constituents (i.e. a geon must maintain its bounded configuration for a sufficient length of time, since otherwise it would not be possible to attribute a structural form to the gravitational geon). Thirdly, it is required that the gravitational field becomes asymptotically flat at spatial infinity. Thus a *gravitational (electromagnetic) geon* is a bounded configuration of gravitational (electromagnetic) waves whose gravity is sufficiently strong to keep them confined on a time-scale which is long compared to the characteristic composing wave period. For the gravitational case, it is required that no matter or fields other than the gravitational field be present.

Through a series of papers, it was established by Anderson and Brill [6] and by CFP that in the high-frequency approximation for a static background metric, the gravitational geon problem and the electromagnetic geon problem are governed by the same set of ordinary differential equations (ODEs) and boundary conditions. These equations are satisfactory for considering the regularity and self-consistency aspects of the geon problem, but not the evolution in time. Any solutions to these equations are necessarily equilibrium solutions since the background metric is assumed to be static. Admissible equilibrium solutions satisfying the boundary conditions have been shown to exist [6]. This paper provides an expanded study of the gravitational and electromagnetic geon problem with particular emphasis upon the dynamic evolution of geon constructs. Section 2 re-examines the numerical solutions to the equations studied in [1] and extends the analysis to obtain information on the 'stability' of these solutions with respect to perturbations of the amplitude eigenvalues. The word 'stability' used in section 2 should be viewed in the context of the boundary conditions of a spatial variable, not a dynamic time variable. Both the analytic behaviour at spatial infinity and the aforementioned stability properties are found by constructing a phase portrait of the ODEs. It is shown explicitly that only unstable equilibrium solutions are possible with respect to perturbations of the amplitude eigenvalues. This result serves to suggest further study of the dynamics (time evolution) of geon constructs.

The evolution in time of electromagnetic geon solutions is studied in section 3. The evolution of the electromagnetic geon is studied instead of the gravitational geon because of the relative ease in computation for the former. With sufficiently high-frequency electromagnetic waves, the results are expected to apply equally well to the gravitational case. The method used is standard perturbation theory modified to accommodate time-averaged fields. The evolution is achieved by applying a small-amplitude time-dependent perturbation to an equilibrium solution and simultaneously solving for the time dependence of the background metric functions. The problem of time averaging the background metric functions can only be solved in a meaningful way if it is assumed that the characteristic frequency of the perturbations vary on a time-scale which is much longer than that of the waves comprising the electromagnetic geon. This is in accordance with the requirement that the background metric be quasi-stable. However, the results of the analysis show that the perturbations must vary on the same time-scale as the constituent waves. This is in contradiction with the original assumption. Hence an internal inconsistency exists when applying perturbation theory to the geon problem. In section 4, the possible interpretations and ramifications of this result are discussed. Since not all of the requirements for existence of a geon are met, it is not possible to conclude that an electromagnetic geon or a gravitational geon is a viable construct. The conclusions are presented in section 5.

2. Phase space analysis

In the high-frequency approximation, the gravitational and electromagnetic geon problem for a static background metric (on time average) reduces to the same set of ordinary differential equations (ODEs) and boundary conditions given by [3–6] (reference [6] corrects sign errors and a difference in normalization found in [5])

$$\phi'' + j\,k\,\phi = 0, \tag{1}$$

$$k' = -\phi^2, \tag{2}$$

$$j' = 3 - k^{-2}\left(1 + \phi'^2\right) \tag{3}$$

and

$$\begin{aligned} &\phi(x) \to 0, \quad k(x) \to 1 \quad \text{and} \quad j(x) \to -\infty \quad \text{for } x \to -\infty, \\ &\phi(x) \to 0, \quad 0 < k(x) < 1 \quad \text{and} \quad j(x) \to -\infty \quad \text{for } x \to \infty, \end{aligned} \tag{4}$$

where x is a radial coordinate and a prime denotes differentiation with respect to x. Therefore, any properties of equations (1)–(3) apply equally well to both the gravitational and electromagnetic geon case. Any solutions to (1)–(3) are necessarily equilibrium solutions since the background metric is assumed to be static. In section 2.1, the numerical solutions presented in [1] will be re-examined. The results suggest further investigation of the numerical solutions is required in order to determine whether the boundary conditions are satisfied. In [6], it was shown that admissible equilibrium solutions to equations (1)–(4) exist. However, the stability of these equilibrium solutions was not studied. The investigation presented in section 2.2 constructs a phase portrait of the ODEs from which both the analytic form at spatial infinity and the stability with respect to perturbations of the amplitude eigenvalues of any solutions will be obtained. Knowledge of solution stability provides a basis for investigating the evolution in time of these solutions. Unlike other investigations [1, 7], we apply a small-amplitude time-dependent perturbation to an equilibrium solution of (1)–(3) for the case of an electromagnetic geon. This is done in section 3. Solving the time-dependent perturbation equations leads to a contradiction with one of the initial assumptions. The contradiction suggests that neither an electromagnetic geon nor a gravitational geon is a viable construct since not all of the requirements for existence of a geon are met. This interpretation of the results obtained from this investigation will be discussed in section 4.

2.1. Numerical integration

Wheeler [1] originally solved the system (1)–(3) by numerical methods in 1955. Since then computer algorithms have evolved considerably for solving differential equations. It is therefore worthwhile to utilize modern techniques† in re-examining those solutions. Even with the algorithm employed in [1] for solving the equations, Wheeler's results are remarkably accurate.

The geon problem (both electromagnetic and gravitational) is reduced to finding a solution to the autonomous system (1)–(3). Admissible solutions to equations (1)–(3) are defined as those $\phi(x)$, $j(x)$ and $k(x)$ that satisfy the following criteria.

(a) *For large negative* x: the wavefunction $\phi(x) \to 0$ and metric function $k(x) \to 1$. Under these conditions $j'(x) \to 2$. If $\phi(x)$, $j(x)$ and $k(x)$ are solutions to the autonomous system (1)–(3), then so are $\phi(x+a)$, $j(x+a)$ and $k(x+a)$ where a is a constant. Choosing the integration constant for $j(x)$ to be zero fixes a and consequently $j(x) \to 2x$. This removes any ambiguity in the start of the integration process. Thus for large negative x, $\phi(x)$ satisfies the equation

$$\frac{\mathrm{d}^2\phi}{\mathrm{d}x^2} = 2x\phi. \tag{5}$$

† To perform the numerical integration, a Fehlberg fourth–fifth order Runge–Kutta method from the MAPLE V R4 program library is used.

The approximate solution to (5) as given in [1] is

$$\phi(x) = \tfrac{1}{3}A(-2x)^{-1/4}\exp\left(-(-2x)^{3/2}\right). \tag{6}$$

(b) *For large positive x*: it is required that $\phi(x) \to 0$, $0 < k(x) < 1$ and $j(x)$ approach large negative values.

The only free parameter is the amplitude A of the wave and this must be chosen so that the solution fits the boundary conditions. The nonlinearity of the problem makes it necessary to integrate the system of equations numerically. The integration is started at $x = -4$. The initial conditions are as follows:

$$\phi(-4) = \phi_0, \tag{7}$$

$$\left.\frac{\mathrm{d}\phi}{\mathrm{d}x}\right|_{x=-4} = \left(\frac{1}{16} + \sqrt{8}\right)\phi_0, \tag{8}$$

$$k(-4) = 1, \tag{9}$$

$$j(-4) = -8, \tag{10}$$

where ϕ_0 is to be chosen to give an admissible solution. Those ϕ_0 values which yield admissible solutions will be referred to as eigenvalues of the system (1)–(3) with initial conditions (7)–(10).

The behaviour for $\phi(x)$ as $x \to \infty$ depends upon the value of ϕ_0 (which translates into an initial choice of the amplitude A). Figure 1 illustrates numerically integrated solutions for values of ϕ_0 given in table 1. Solution set 1 shows that for sufficiently large values of ϕ_0, $\phi(x)$ reaches a positive minimum and then increases exponentially. As ϕ_0 is allowed to decrease, the exponential growth of $\phi(x)$ is delayed. This is depicted by solution sets 2 and 3. A further

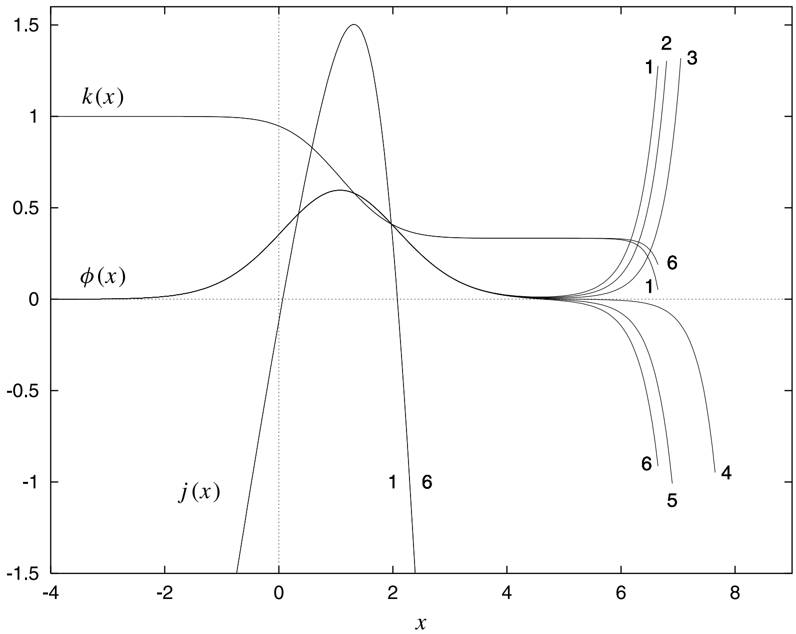

Figure 1. Results of the numerical integration for the geon differential equations (1)–(3). The values of ϕ_0 for solution sets 1–6 are summarized in table 1. The integration started at $x = -4$ and could not proceed beyond $x \simeq 7$ for the given initial values. The active region begins at $x \simeq 0.12$ and ends at $x \simeq 2.13$. A possible admissible solution lies between sets 3 and 4. Note that for $j(x)$, curves 1–6 are indistinguishable.

Table 1. Values of ϕ_0 for solution sets 1–6.

Solution set	ϕ_0
1	9.7910×10^{-5}
2	9.7908×10^{-5}
3	9.7906×10^{-5}
4	9.7904×10^{-5}
5	9.7902×10^{-5}
6	9.7900×10^{-5}

reduction in ϕ_0 results in $\phi(x) \to -\infty$ exponentially as shown in solution sets 4–6. A possible admissible solution lies between solution sets 3 and 4.

The mass of the geon inside radius ρ is related to the function $k(x)$ in the following way:

$$M(\rho(x)) = \frac{1}{b}\lambda_0(x) = \frac{1}{2b}\left(1 - k^2\right), \tag{11}$$

with $b = 1/Q_1(\infty) = k(\infty)$. This implies that

$$0 < k^2(x) \leqslant 1 \qquad \text{as} \quad x \to \infty \tag{12}$$

in order to have a positive total mass. The mass factor $k(x)$ gives a positive mass throughout the integrable region and appears to have a $k(\infty)$ value of approximately $1/3$. The 'active region' can be identified in the x coordinate system as the region where the function $j(x)$ is positive. In this region, the function $\phi(x)$ has oscillatory behaviour. The function $j(x)$ is positive only for a limited range in the neighbourhood of $x = 1$, thus identifying the active region. In figure 1, the active region begins at $x \simeq 0.12$ and ends at $x \simeq 2.13$. The first admissible solution (characterized by $\phi(x)$ having one local maximum and no local minima) appears to lie between those values of ϕ_0 in the range $9.7904 \times 10^{-5} < \phi_0 < 9.7906 \times 10^{-5}$. Qualitatively, these results are similar to those in [1]. The only main difference between the calculation of [1] and the present one is that in [1], the first admissible solution appears to lie in the range $1.030\,00 \times 10^{-4} < \phi_0 < 1.031\,25 \times 10^{-4}$ and the active region starts at $x \simeq 4.05$ and ends at $x \simeq 6.02$.

2.2. Existence and stability of equilibrium states

We are interested in determining the analytical behaviour of the solutions shown in figure 1 as $x \to \infty$. By constructing the phase portrait for the differential equations, it will be possible to determine both the existence and stability properties of potential admissible solutions. We start by rewriting equations (1)–(3) as the set of first-order equations

$$u' = -j\,k\,\phi, \tag{13}$$
$$\phi' = u, \tag{14}$$
$$k' = -\phi^2, \tag{15}$$
$$j' = 3 - k^{-2} + u^2 k^{-2}. \tag{16}$$

It is sufficient to look for solutions with the properties

$$\left.\begin{array}{l} \phi,\, u \to 0 \\ k \to 1 \end{array}\right\} \qquad \text{as} \quad x \to -\infty, \qquad \left.\begin{array}{l} \phi,\, u \to 0 \\ k \to \text{constant} > 0 \end{array}\right\} \qquad \text{as} \quad x \to +\infty \tag{17}$$

and j remains finite for finite x. In a phase space, the critical points (or equilibrium points) are characterized by those points where the derivatives of u, ϕ, k and j are zero. The analytic behaviour of the solution about a critical point is determined by analysing the corresponding linear system in a neighbourhood of that critical point [8].

The first step is to obtain the critical points of the system (13)–(16). One can easily verify that

$$u = 0, \tag{18}$$

$$\phi = 0, \tag{19}$$

$$k = \pm\frac{1}{\sqrt{3}} \tag{20}$$

is sufficient to satisfy $u' = \phi' = k' = j' = 0$. Thus the coordinates of the critical point in the phase space are

$$u = 0, \tag{21}$$

$$\phi = 0, \tag{22}$$

$$k = \frac{1}{\sqrt{3}}, \tag{23}$$

$$j = s, \qquad s \in \mathbb{R}, \tag{24}$$

where s is any value of $j(x)$. The function $k(x)$ cannot pass through zero since equation (3) becomes singular. The positive root of equation (20) is chosen to ensure positive $k(x)$, since initially $k(-\infty) = 1$. It is useful to shift the critical point to the origin using the following transformation:

$$\begin{aligned} \phi(x) &= f_1(x), & u(x) &= f_2(x), \\ k(x) &= f_3(x) + \frac{1}{\sqrt{3}}, & j(x) &= f_4(x) + s. \end{aligned} \tag{25}$$

Therefore, the field equations become

$$f_1' = f_2, \tag{26}$$

$$f_2' = -\left(f_4 + s\right)\left(f_3 + \frac{1}{\sqrt{3}}\right) f_1, \tag{27}$$

$$f_3' = -f_1^2, \tag{28}$$

$$f_4' = 3 - \left(1 + f_2^2\right)\left(f_3 + \frac{1}{\sqrt{3}}\right)^{-2}, \tag{29}$$

with the critical point at $f_1 = f_2 = f_3 = f_4 = 0$. To linearize the field equations about this critical point, a MacLaurin series of $f_i' = f_i'(f_1, f_2, f_3, f_4)$, $i = 1, \ldots, 4$ is taken to first order and evaluated at the critical point (denoted by cp below), i.e.

$$f_i' = f_i'\big|_{\mathrm{cp}} + \left.\frac{\partial f_i'}{\partial f_1}\right|_{\mathrm{cp}} f_1 + \left.\frac{\partial f_i'}{\partial f_2}\right|_{\mathrm{cp}} f_2 + \left.\frac{\partial f_i'}{\partial f_3}\right|_{\mathrm{cp}} f_3 + \left.\frac{\partial f_i'}{\partial f_4}\right|_{\mathrm{cp}} f_4 + \cdots. \tag{30}$$

Written in matrix form, the linearized field equations are

$$\frac{\mathrm{d}\boldsymbol{w}}{\mathrm{d}x} = \mathbf{M}\,\boldsymbol{w}, \tag{31}$$

where

$$\boldsymbol{w} = \begin{pmatrix} f_1 \\ f_2 \\ f_3 \\ f_4 \end{pmatrix} \qquad \text{and} \qquad \mathbf{M} = \begin{pmatrix} 0 & 1 & 0 & 0 \\ -s/\sqrt{3} & 0 & 0 & 0 \\ 0 & 0 & 0 & 0 \\ 0 & 0 & 6\sqrt{3} & 0 \end{pmatrix}. \tag{32}$$

The general solution to the above matrix differential equation is the eigenvector

$$\boldsymbol{w} = c_1 \begin{pmatrix} 0 \\ 0 \\ 0 \\ 1 \end{pmatrix} + c_2 \left[\begin{pmatrix} 0 \\ 0 \\ 0 \\ 1 \end{pmatrix} x + \begin{pmatrix} 0 \\ 0 \\ \sqrt{3}/18 \\ 0 \end{pmatrix} \right] + c_3 \begin{pmatrix} 1 \\ \alpha \\ 0 \\ 0 \end{pmatrix} \mathrm{e}^{\alpha x} + c_4 \begin{pmatrix} 1 \\ -\alpha \\ 0 \\ 0 \end{pmatrix} \mathrm{e}^{-\alpha x}, \tag{33}$$

where $\alpha \equiv \sqrt{-s/\sqrt{3}}$ and $c_i,\ i = 1, \ldots, 4$ are constants. Therefore, the solution to the linear system is

$$f_1(x) = c_3\, \mathrm{e}^{\alpha x} + c_4\, \mathrm{e}^{-\alpha x}, \tag{34}$$

$$f_2(x) = c_3\, \alpha\, \mathrm{e}^{\alpha x} - c_4\, \alpha\, \mathrm{e}^{-\alpha x}, \tag{35}$$

$$f_3(x) = \tfrac{1}{18}\sqrt{3}\, c_2, \tag{36}$$

$$f_4(x) = c_1 + c_2\, x. \tag{37}$$

The eigenvector $\boldsymbol{w}$ shows that in a neighbourhood of the critical point, the nonlinear system decouples into the disjoint subspaces $(f_1,\ f_2)$ and $(f_3,\ f_4)$.

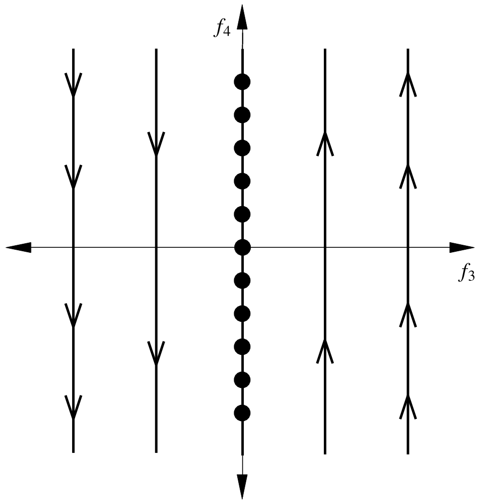

Figure 2. The $(f_3,\ f_4)$ phase space projection illustrates a non-isolated critical point. The critical point under investigation is located at the origin. The f_4-axis is a continuous set of critical points in a neighbourhood of the origin. The functions $f_4 \propto j$ and $f_3 \propto k$ behave as a linear function of x and a constant function, respectively, in a neighbourhood of the critical point not on the f_4-axis.

The phase space projection of $(f_3,\ f_4)$ (which is proportional to $(k,\ j)$) is illustrated in figure 2. Since s can take any value of j, the critical point lies at an arbitrary position $s \leqslant \max(j)$ on the curve $k(x) = (\sqrt{3}/18)\, c_2 + (1/\sqrt{3})$ which is transformed back to the origin in the (f_3, f_4) subspace. Equations (36) and (37) show that in a neighbourhood of the critical point, but not on the f_4-axis, f_3 and f_4 behave as a constant and a linear function of x, respectively. If one is on the f_4-axis in a neighbourhood of the critical point, then $c_2 = 0$. Hence $f_4 = c_1$ defines a continuous set of critical points. These critical points are examples of non-isolated critical points. The $(f_3,\ f_4)$ projection is insufficient for determining the existence and stability of admissible solutions since it only gives information about the functions j and k.

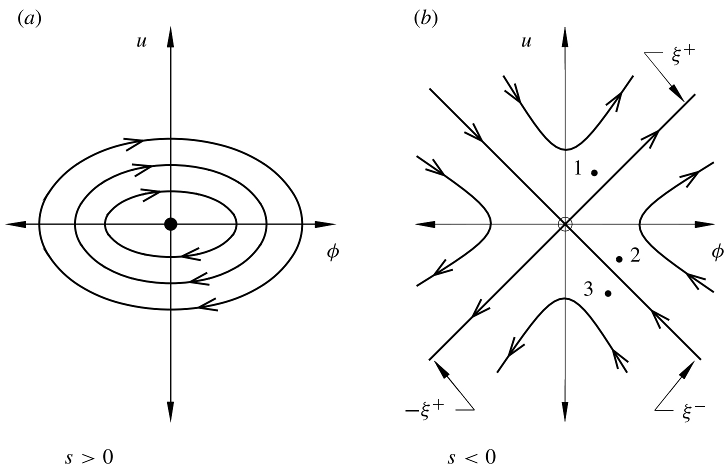

Figure 3. (*a*) Illustration of a stable critical point. This type of critical point occurs when the value of the parameter $s > 0$. (*b*) Illustration of an unstable critical point. This type of critical point occurs when the value of the parameter $s < 0$.

The nature of the $(f_1,\ f_2)$ subspace† (or the $(\phi,\ u)$ subspace) depends upon the parameter $s \in j$. It will determine the stability properties with respect to perturbations of the amplitude eigenvalues of any admissible solutions. However, a three-dimensional phase space projection in the coordinates $(\phi,\ u,\ j)$ is necessary to determine the existence of admissible solutions. Illustrations of the two possible phase space projections of $(\phi,\ u)$ are shown in figure 3. Examining (34) and (35), if $s > 0$, then ϕ and u behave as sinusoidal functions of x. This type of critical point is described as a centre (figure 3(*a*)) and is a *stable* critical point. If $s < 0$, then ϕ and u have an exponential behaviour and the critical point is *unstable*. This type of critical point is described as a saddle point (figure 3(*b*)). By following the integration procedure in the parameter x for solution sets 1 and 6 of figure 1, the behaviour of the complete nonlinear system can be described.

Figure 4 shows the three-dimensional $(\phi,\ u,\ j)$ phase space projection of solution sets 1 and 6. The integration procedure starts in plane B of figure 4 at $j = -8$. In addition, the solution trajectories start somewhere along the line $u = (\frac{1}{16} + \sqrt{8})\phi_0$, which must necessarily lie to the left of the unstable asymptote ξ^+. One such point is labelled '1' in figure 3(*b*). In order for the system to satisfy the boundary conditions (17), it is necessary for at least one solution to flow along the unstable asymptote ξ^- (in the $j = s \to -\infty$ plane). If figure 3(*b*) were a complete description of the phase space, then it would be impossible for a solution starting at position '1' to cross ξ^+. This is a consequence of the well known property of autonomous systems that phase space trajectories do not cross. However, as the integration process in x continues, the value of j increases from a negative value to a positive value. Therefore, the nature of the critical point in the two-dimensional $(\phi,\ u)$ phase planes changes temporarily from a saddle point to that of a centre. Plane A of figure 4 is an illustration of one such critical point. Soon afterward, j decreases to negative values and the critical points are saddle points once again. However, the solution trajectories have crossed ξ^+ and now follow the flow along the unstable asymptote ξ^-. Upon the transition of the critical points from centres to saddle points, the asymptotes have been re-established with solution sets 1 and 6 on opposite sides of

† It is convenient to use the functions ϕ, u in place of f_1, f_2 for the remainder of this section. Recall that $\phi = f_1$, $u = f_2$ from equation (25).

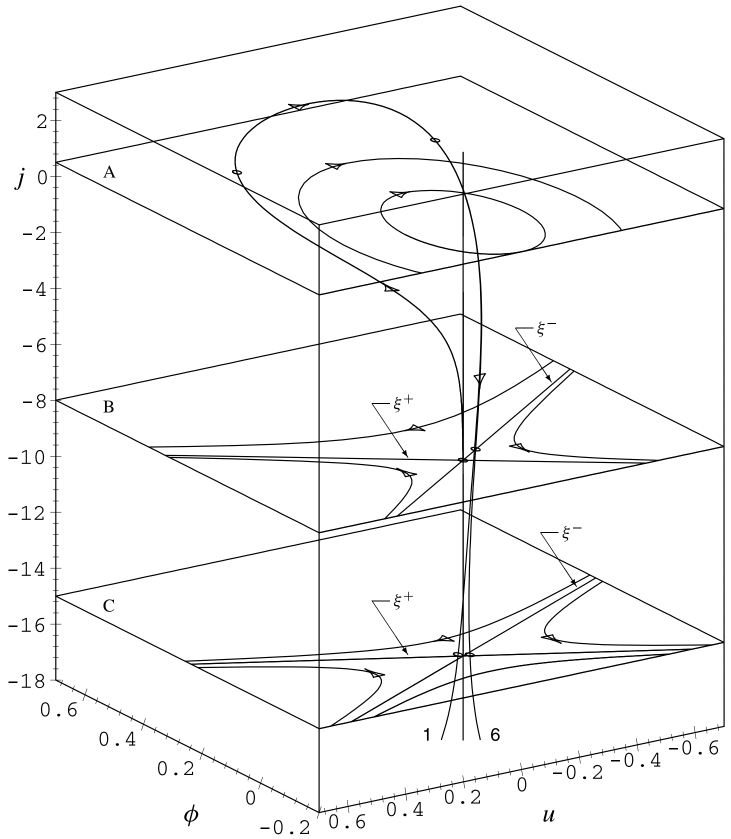

Figure 4. The three-dimensional $(\phi,\ u,\ j)$ projection of the phase space curves for the numerical solution sets 1 and 6 shown in figure 1. The numerical integration starts in plane B, proceeds up through plane A and continues down through plane C. The nature of the critical points along the j-axis (origin of the $(\phi,\ u)$ planes) change from centres ($j > 0$) to saddle points ($j < 0$) demonstrating the system instability.

the ξ^- asymptote. The positions where solution sets 1 and 6 cut the $(\phi,\ u)$ planes for $j < 0$ are schematically illustrated as points '2' and '3' respectively, in figure 3(*b*). In figure 4, these positions are most clearly seen in plane C. Since trajectories for autonomous systems do not cross and the trajectories depend continuously on the initial data, there must be a value of ϕ_0 for which the trajectory approaches ξ^- as $j = s \to -\infty$. The existence of this trajectory shows that it is possible to find an eigenvalue of ϕ_0 which satisfies the boundary conditions (17). However, the nature of the critical point as $j = s \to -\infty$ ($x \to \infty$) is a saddle point and therefore this eigenvalue solution is an unstable solution. Since solution set 1 cuts plane C at position '2' of figure 3(*b*), the flow of the integration process requires this set to approach ξ^+. Similarly, solution set 6 must approach ξ^-, since it cuts plane C at position '3'. Hence, any small perturbation of the eigenvalue of ϕ_0 implies the constant $c_3 \neq 0$ in (34) and (35). Thus the non-eigenvalue solutions do not satisfy the boundary conditions. Figure 5 shows the $(\phi,\ u)$ subspace for the six solution sets of figure 1. The projection is for $j < -15$. A comparison of figure 5 to figure 3(*b*) confirms that the admissible solution is unstable.

The existence of admissible solutions and instability of the electromagnetic geon system were discussed in [1]. However, it was based on the numerical solution curves similar to

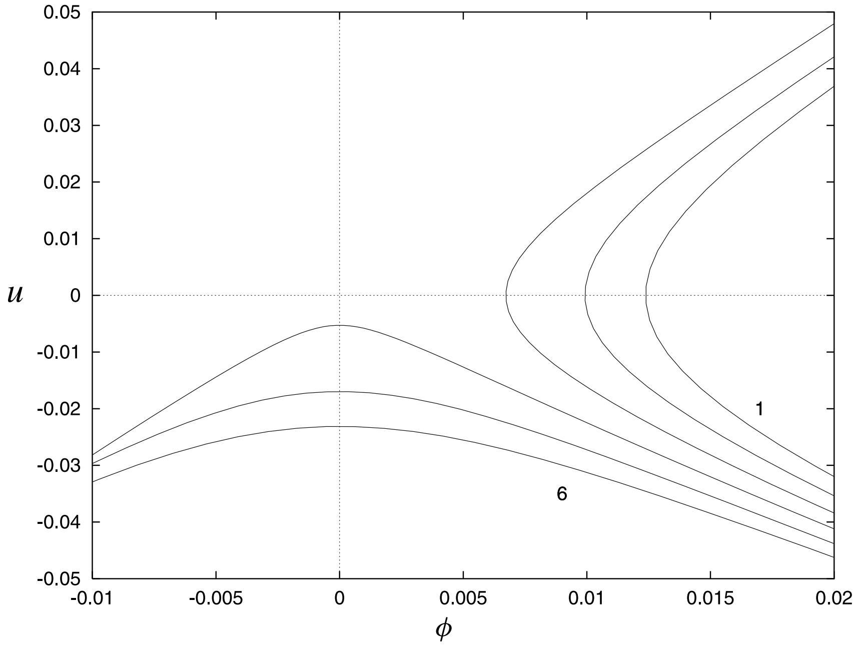

Figure 5. The (ϕ, u) phase space projection of solution sets 1–6 for $j < -15$. It has the characteristics of figure 3(*b*). This indicates that the critical point at the origin is unstable as $j \to -\infty$.

figure 1. Performing a phase portrait analysis, we have formally shown that an eigenvalue does exist† which satisfies conditions (17). We have also shown that this solution must necessarily be *unstable* with respect to perturbations of the eigenvalue of ϕ_0. This result suggests that geon constructs are dynamically unstable, i.e. the ensemble of waves must collapse or explode. In [1], it was also suggested that a spherical geon would most likely collapse to a toroidal geon [9], presumably thought to be more stable. It was argued by Ernst [9] that the construction of a toroidal geon could be realized if one had complete knowledge of a linear geon (which approximates a small segment of the toroidal geon). Numerical evidence for amplitude eigenvalues in analogy with the spherical geon were presented in [9]. This work was extended in [10] by performing a phase portrait analysis. It was found that only unstable admissible solutions exist, as in the case of the spherical geon. It has been suggested [6] that this is sufficient for proclaiming the existence of both types of geons (electromagnetic and gravitational). However, in section 1, it was noted that a true geon must have the property that the ensemble of waves comprising the geon be confined on a time-scale much longer than the typical period of the constituent waves. Otherwise it would not be possible to attribute a structural form to the geon. What is yet to be determined analytically is the dynamic behaviour of geon constructs when perturbations are present. The next section presents a time-dependent perturbation analysis of the equations that describe the electromagnetic geon in an attempt to determine this time-scale.

† Existence of the eigenvalue was derived independently in [6] using an alternate method. However, stability aspects were not discussed in [6].

3. Time-evolution analysis of the electromagnetic geon

The electromagnetic geon model employed in [1] assumed a background metric which is independent of time. This precludes the possibility of studying the time evolution of the individual modes coupled to a time-evolving background metric. Instead of introducing a time dependence into the system of equations and solving the coupled wave–background system, an alternate method was employed in [1] for determining the time-scale of the collapse or 'lifetime' of the electromagnetic geon. It was based on an alpha-decay model of barrier potential penetration. The quantum mechanical nature of alpha decay brings into question the validity of using such a model for determining the lifetime of a classical object such as a geon [10]. There are known phenomena which represent classical wave penetration of a potential barrier. For example, the optical phenomenon of frustrated total internal reflection [11] is such a process. It is important to note that in both alpha decay and frustrated total internal reflection, the potential is supplied by some material and not the waves themselves, as is necessary for the case of geons. Whether the analogy exists between these examples of barrier penetration and the time evolution of a geon based upon the coupled Einstein–Maxwell equations is the subject of this section.

Another approach towards determining the lifetime of an electromagnetic geon is that of Brill [7]. The method is to study the evolution of the ensemble of photons which produce the effective potential using a thin-shell model for the electromagnetic geon. It was found that the radial position of the thin shell underwent a displacement towards collapse. It was also stated that the rate of collapse was 'slow'.

The junction condition problems associated with analysing thin-shell geon models has previously been discussed in some detail in [5]. In addition, the evolution of the thin-shell model in [7] does not allow for leakage of radiation during the collapse nor does it allow an evolving shell thickness (evolving active region) as one might expect. The effect of correcting these deficiencies on the rate of collapse is not clear. A full understanding of the evolution of a geon must take into account the evolution of the typical individual modes of vibration coupled to the evolution of the collective ensemble of waves in a singularity-free model.

It is evident that models for studying the evolution of geons must be based on solving the Einstein (or Einstein–Maxwell) field equations. Intuitive models are not sufficient for describing the true physical system. To avoid the interpretation problems associated with the alpha-decay and thin-shell models and correct for the deficiencies of each model, the derivation of the electromagnetic geon equations [1] will be modified to permit the study of the time evolution of the electromagnetic geon. The electromagnetic geon will be studied instead of the gravitational geon because of the relative ease in computation for the former. Equilibrium solutions for the gravitational and electromagnetic geon are governed by the same set of ODEs. Therefore, it is not expected that the modified gravitational geon equations in the high-frequency approximation would yield a significantly different result from the electromagnetic case.

We are interested in following the evolution of the electromagnetic geon in the radial direction. Observing the time evolution of the metric reflects the evolution of the ensemble of electromagnetic waves comprising the geon. However, it is not sufficient to simply perturb the background metric functions. It is the electromagnetic waves which are the source for the gravitational field, hence both the gravitational and electromagnetic quantities must be perturbed. This will be done by applying an amplitude perturbation on the electromagnetic waves comprising the geon in such a way as to induce the background metric to evolve in time. Frequency perturbations are not explicitly considered in the following derivation for two main reasons. Firstly, the stability analysis of the previous section indicates that the instability of the admissible equilibrium solution originates from changes in the amplitude eigenvalue (initial condition). Secondly, it can be shown that a perturbation of the form $\Omega \to \Omega + \delta\Omega$ (where Ω is the characteristic frequency of the electromagnetic waves) is a special case of the amplitude perturbation studied below. Restricting study to the radial direction maintains the field equations in their simplest form. It should be emphasized that the time–space average of the electromagnetic disturbance must be incorporated into the background metric equations to maintain spherical symmetry, but still allow for the solution to evolve in time. This time-averaging problem will be addressed when the perturbation is applied. Before the perturbation analysis is performed, the angle-averaged time-dependent electromagnetic geon field equations must first be derived. This part of the derivation follows closely that of [1].

The equations presented below are derived in greater detail in appendix A. Only an outline of the derivation is given here. We start by defining the electromagnetic vector potential for one mode of the electromagnetic waves

$$A_\mu = \left(0,\ 0,\ 0,\ A_\varphi\right), \tag{38}$$

where

$$A_\varphi = a(r,t)B(\theta), \qquad B(\theta) = \sin\theta \frac{\mathrm{d}}{\mathrm{d}\theta} P_l(\cos\theta). \tag{39}$$

The function $a(r,t)$ has been left unspecified at this stage. The time-dependent background metric is

$$\mathrm{d}s^2 = g_{\alpha\beta}\,\mathrm{d}x^\alpha\,\mathrm{d}x^\beta = -\mathrm{e}^\nu\,\mathrm{d}t^2 + \mathrm{e}^\lambda\,\mathrm{d}r^2 + r^2\,\mathrm{d}\theta^2 + r^2\sin^2\theta\,\mathrm{d}\varphi^2, \tag{40}$$

where

$$\nu = \nu(r,t), \qquad \lambda = \lambda(r,t).$$

In the absence of charges and currents, Maxwell's equations in a curved spacetime are

$$\frac{1}{\sqrt{-g}}\frac{\partial}{\partial x^\alpha}\left(\sqrt{-g}F^{\beta\alpha}\right) = 0, \tag{41}$$

$$F_{\alpha\beta,\gamma} + F_{\gamma\alpha,\beta} + F_{\beta\gamma,\alpha} = 0, \tag{42}$$

where g is the determinant of the metric (40) and the Maxwell tensor, $F_{\alpha\beta}$, is related to the 4-vector potential as $F_{\alpha\beta} = A_{\beta,\alpha} - A_{\alpha,\beta}$. The Einstein equations for the electromagnetic geon are

$$G_\mu{}^\nu = 8\pi\left\langle T_\mu{}^\nu\right\rangle, \tag{43}$$

where $\langle\cdot\rangle$ denotes a time–space average over all N active modes† of the electromagnetic waves. Substituting (38) into (41) and (43), taking the angle average and finally transforming to the $\rho = \Omega r$ coordinate system yields the wave equation

$$\Omega^2\frac{\partial^2 a}{\partial\rho^{*2}} - \Omega^2 l^{*2}\rho^{-2}\left(1-\frac{2L}{\rho}\right)Q^2 a - \left(1-\frac{2L}{\rho}\right)^2 Q^2\frac{\partial^2 a}{\partial t^{*2}} = 0 \tag{44}$$

† The active modes are characterized by a sequence of parameter values (a family of modes) for which the effective stress–energy is concentrated in the same spatial region.

and the background field equations

$$\frac{\partial L}{\partial \rho^*} = \frac{\kappa_l^2}{2}\left(Q^{-1}\left(\Omega^2\left\langle\left(\frac{\partial a}{\partial \rho^*}\right)^2\right\rangle_{\mathrm{T}} + \left\langle\left(\frac{\partial a}{\partial t}\right)^2\right\rangle_{\mathrm{T}}\right) + \Omega^2 l^{*2}\rho^{-2}\left(1-\frac{2L}{\rho}\right)Q\left\langle a^2\right\rangle_{\mathrm{T}}\right), \quad (45)$$

$$\frac{\partial Q}{\partial \rho^*} = \frac{\kappa_l^2}{\rho - 2L}\left(\Omega^2\left\langle\left(\frac{\partial a}{\partial \rho^*}\right)^2\right\rangle_{\mathrm{T}} + \left\langle\left(\frac{\partial a}{\partial \rho^*}\right)^2\right\rangle_{\mathrm{T}}\right), \quad (46)$$

$$\frac{\partial L}{\partial t} = \kappa_l^2\Omega^2 Q^{-1}\left\langle\frac{\partial a}{\partial \rho^*}\frac{\partial a}{\partial t}\right\rangle_{\mathrm{T}}, \quad (47)$$

where

$$\frac{\partial}{\partial \rho^*} \equiv \left(1-\frac{2L}{\rho}\right)Q\frac{\partial}{\partial \rho}, \quad (48)$$

$$\frac{\partial^2}{\partial t^{*2}} = \left(1-\frac{2L}{\rho}\right)^{-1} Q^{-1}\frac{\partial}{\partial t}\left(\left(1-\frac{2L}{\rho}\right)^{-1} Q^{-1}\frac{\partial}{\partial t}\right), \quad (49)$$

and

$$\kappa_l \equiv \sqrt{\frac{Nl^{*2}}{2l+1}} \qquad l^* \equiv \sqrt{l(l+1)}. \quad (50)$$

In the above equations $L(\rho)$ and $Q(\rho)$ are metric functions (see equations (A24) and (A25)) and the symbol $\langle\cdot\rangle_{\mathrm{T}}$ denotes a time average is to be taken. Equations (44)–(47) are the starting point for developing the dynamic perturbation (time-evolution) equations. The $\partial Q/\partial t$ equation (found from the $G_\theta{}^\theta = 8\pi\left\langle T_\theta{}^\theta\right\rangle$ equation) is not used in the subsequent analysis, but is given in appendix A for completeness.

The time-averaged equilibrium solution in [1] has the form

$$\kappa_l\,\Omega\, a(\rho,\ t) = f_0(\rho)\sin\Omega t, \quad (51)$$

$$L(\rho,\ t) = L_0(\rho), \quad (52)$$

$$Q(\rho,\ t) = Q_0(\rho), \quad (53)$$

where $f_0(\rho)$, $L_0(\rho)$ and $Q_0(\rho)$ are known functions†. We will designate this as the 'unperturbed solution'. Two general forms for the radial perturbation of the wavefunction $a(\rho,\ t)$ will be considered. The first is given by

$$\kappa_l\,\Omega\, a(\rho,\ t) = f_0(\rho)\sin\Omega t + \delta u_1(\rho,\ t) + \delta^2 u_2(\rho,\ t) + \mathrm{O}\left(\delta^3\right), \qquad \delta \ll 1, \quad (54)$$

where δ is the expansion parameter. (Note that the addition of a phase constant to $\sin\Omega t$ does not affect the results which follow. Thus the phase constant is set to zero.) As a result, a small time-dependent perturbation is introduced in the metric functions,

$$L(\rho,\ t) = L_0(\rho) + \delta L_1(\rho,\ t) + \delta^2 L_2(\rho,\ t) + \mathrm{O}\left(\delta^3\right), \quad (55)$$

$$Q(\rho,\ t) = Q_0(\rho) + \delta Q_1(\rho,\ t) + \delta^2 Q_2(\rho,\ t) + \mathrm{O}\left(\delta^3\right). \quad (56)$$

The perturbation expansion will be carried out to the first order in δ. Before the perturbed system is solved in a self-consistent manner, the problem of time averaging the functions on

† These are known as numerical solutions to the system (1)–(3) with initial conditions (7)–(10) in the high angular momentum approximation.

the right-hand side of equations (45)–(47) must be addressed. From the definition of a time average and equation (54),

$$\begin{aligned}\kappa_l^2\,\Omega^2\left\langle a^2(\rho,\ t)\right\rangle_{\mathrm{T}} &\equiv \frac{1}{T}\int_0^T \kappa_l^2\Omega^2 a^2(\rho,\ t)\,\mathrm{d}t\\ &= \frac{1}{2}f_0^2(\rho) + \frac{1}{T}\int_0^T \big(2\delta u_1(\rho,\ t)\,f_0(\rho)\sin\Omega\,t\\ &\quad + \delta^2\left(u_1^2(\rho,\ t) + 2u_2(\rho,\ t)\,f_0(\rho)\sin\Omega\,t\right) + \mathrm{O}\left(\delta^3\right)\big)\,\mathrm{d}t,\end{aligned} \tag{57}$$

where $T = 2\pi\Omega^{-1}$ is the period of the electromagnetic waves. In order to develop the perturbation analysis, it is necessary to make some assumptions about the function $u_1(\rho, t)$. The presence of unevaluated integrals on the right-hand side of the differential equations (45)–(47) would not make it possible to proceed with the analysis beyond this point. Let us suppose that the time dependence of $u_1(\rho, t)$ was sinusoidal and its characteristic frequency was of the order Ω of the electromagnetic waves. In this case, the time dependence is lost to all orders in δ upon time averaging. In essence, this assumption on $u_1(\rho,\ t)$ precludes the possibility of a time-dependent evolution of the system. This is not satisfactory. To maintain a time dependence after time averaging, another time-scale will be introduced into the problem. Suppose the time dependence of $u_1(\rho, t)$ was again sinusoidal and its characteristic frequency was of the order $\omega \ll \Omega$. In this case, $u_1(\rho, t)$ is approximately constant over the short time period $T = 2\pi\Omega^{-1}$ of the electromagnetic waves and thus is constant in the time-average integral. Evaluating the time average of $a^2(\rho,\ t)$ under this assumption yields

$$\begin{aligned}\kappa_l^2\,\Omega^2\left\langle a^2(\rho,\ t)\right\rangle_{\mathrm{T}} = \frac{1}{T}\int_0^T &\big(f_0^2(\rho)\sin^2\Omega\,t + 2\delta\,u_1(\rho,\ t)\,f_0(\rho)\sin\Omega\,t\\ &+\delta^2\left(u_1^2(\rho,\ t) + 2u_2(\rho,\ t)\,f_0(\rho)\sin\Omega\,t\right)\big)\,\mathrm{d}t + \mathrm{O}\left(\delta^3\right)\\ = \tfrac{1}{2}f_0^2(\rho) &+ \delta^2 u_1^2(\rho,\ t) + \mathrm{O}\left(\delta^3\right).\end{aligned} \tag{58}$$

Therefore, the time dependence is not present until the second order in δ. This is sufficient to proceed with the time evolution of the system, since each order in the expansion parameter δ must be set to zero. To *first* order in δ

$$\kappa_l^2\,\Omega^2\left\langle a^2(\rho,\ t)\right\rangle_{\mathrm{T}} = \tfrac{1}{2}f_0^2 + \mathrm{O}\left(\delta^2\right). \tag{59}$$

Similarly, the remaining time averages are

$$\kappa_l^2\,\Omega^2\left\langle\left(\frac{\partial a}{\partial\rho^*}\right)^2\right\rangle_{\mathrm{T}} = \frac{1}{2}\left(\frac{\mathrm{d}f_0}{\mathrm{d}\rho^*}\right)^2 + \mathrm{O}\left(\delta^2\right), \tag{60}$$

$$\kappa_l^2\,\Omega^2\left\langle\left(\frac{\partial a}{\partial t}\right)^2\right\rangle_{\mathrm{T}} = \tfrac{1}{2}\Omega^2 f_0^2 + \mathrm{O}\left(\delta^2\right), \tag{61}$$

$$\kappa_l^2\,\Omega^2\left\langle\frac{\partial a}{\partial t}\frac{\partial a}{\partial\rho^*}\right\rangle_{\mathrm{T}} = \mathrm{O}\left(\delta^2\right). \tag{62}$$

Substitution of (54)–(62) into (44)–(47), expanding to first order in δ and setting each order in δ to zero yields the unperturbed equations (63)–(65). The properties of the unperturbed equations

$$\frac{\mathrm{d}^2 f_0}{\mathrm{d}\rho^{*2}} + \left(1 - l^{*2} Q_0^2 \rho^{-2}\left(1 - \frac{2L_0}{\rho}\right)\right) f_0 = 0, \tag{63}$$

$$\frac{\mathrm{d}L_0}{\mathrm{d}\rho^*} = \frac{1}{2Q_0}\left(f_0^2 + \left(\frac{\mathrm{d}f_0}{\mathrm{d}\rho^*}\right)^2 + l^{*2} Q_0^2 \rho^{-2}\left(1 - \frac{2L_0}{\rho}\right) f_0^2\right), \tag{64}$$

$$\frac{\mathrm{d}Q_0}{\mathrm{d}\rho^*} = (\rho - 2L_0)^{-1}\left(f_0^2 + \left(\frac{\mathrm{d}f_0}{\mathrm{d}\rho^*}\right)^2\right), \tag{65}$$

are known from [1] and therefore can be used in the analysis of the first-order equations. Setting the first-order part of the wave equation (44) to zero yields

$$A(\rho,\, t)\sin\Omega t + B(\rho,\, t)\cos\Omega t + C(\rho,\, t) = 0, \tag{66}$$

where

$$\begin{aligned}
A(\rho,\, t) \equiv \Omega\Bigg(&\left(Q_1(\rho,\, t)\left(1 - \frac{2L_0}{\rho}\right) - 2\rho^{-1}L_1(\rho,\, t)Q_0\right)\\
&\times\left(2\rho^{-2}Q_0\frac{\mathrm{d}f_0}{\mathrm{d}\rho}\left(L_0 - \rho\frac{\mathrm{d}L_0}{\mathrm{d}\rho}\right) + Q_0\frac{\mathrm{d}^2 f_0}{\mathrm{d}\rho^2}\left(1 - \frac{2L_0}{\rho}\right)\right.\\
&\left.+\frac{\mathrm{d}f_0}{\mathrm{d}\rho}\frac{\mathrm{d}Q_0}{\mathrm{d}\rho}\left(1 - \frac{2L_0}{\rho}\right)\right)\\
&+2\rho^{-3}l^{*2}Q_0\left(Q_0L_1(\rho,\, t) - \rho Q_1(\rho,\, t)\left(1 - \frac{2L_0}{\rho}\right)\right) f_0 + Q_0\left(1 - \frac{2L_0}{\rho}\right)\\
&\times\left(2\rho^{-2}\frac{\mathrm{d}f_0}{\mathrm{d}\rho}\left(Q_1\left(L_0 - \rho\frac{\mathrm{d}L_0}{\mathrm{d}\rho}\right) + Q_0\left(L_1(\rho,\, t) - \rho\frac{\partial}{\partial\rho}L_1(\rho,\, t)\right)\right)\right.\\
&+\left(\left(1 - \frac{2L_0}{\rho}\right)\frac{\partial}{\partial\rho}Q_1(\rho,\, t) - 2\rho^{-1}L_1(\rho,\, t)\frac{\mathrm{d}Q_0}{\mathrm{d}\rho}\right)\frac{\mathrm{d}f_0}{\mathrm{d}\rho}\\
&+\left(Q_1(\rho,\, t)\left(1 - \frac{2L_0}{\rho}\right) - 2\rho^{-1}L_1(\rho,\, t)Q_0\right)\frac{\mathrm{d}^2 f_0}{\mathrm{d}\rho^2}\\
&+\frac{f_0}{\rho - 2L_0}\left(2L_1(\rho,\, t) - \rho\left(1 - \frac{2L_0}{\rho}\right)Q_0^{-1}Q_1(\rho,\, t)\right)\\
&\left.+\left(1 - \frac{2L_0}{\rho}\right)^{-1}Q_0^{-1}\left(Q_1(\rho,\, t)\left(1 - \frac{2L_0}{\rho}\right) - 2\rho^{-1}L_1(\rho,\, t)Q_0\right) f_0\right),
\end{aligned} \tag{67}$$

$$B(\rho,\, t) \equiv f_0\left(2\rho^{-1}\left(1 - \frac{2L_0}{\rho}\right)^{-1}\frac{\partial}{\partial t}L_1(\rho,\, t) - Q_0^{-1}\frac{\partial}{\partial t}Q_1(\rho,\, t)\right) \tag{68}$$

and

$$C(\rho,\, t) \equiv \frac{\partial^2}{\partial\rho^{*2}}u_1(\rho,\, t) - l^{*2}Q_0^2\rho^{-2}\left(1 - \frac{2L_0}{\rho}\right)u_1(\rho,\, t) - \Omega^{-2}\frac{\partial^2}{\partial t^2}u_1(\rho,\, t). \tag{69}$$

In order to satisfy the first-order wave equation (66), the conditions $A(\rho,\, t) = 0$, $B(\rho,\, t) = 0$ and $C(\rho,\, t) = 0$ must be imposed. This is justified since $\sin\Omega t$ and $\cos\Omega t$ are independent functions in the approximation where $A(\rho,\, t)$, $B(\rho,\, t)$ and $C(\rho,\, t)$ are slowly varying functions of time. We will focus upon the latter equation, since it is the simplest of the three equations. Setting (69) to zero yields the equation

$$\frac{\partial^2}{\partial\rho^{*2}}u_1(\rho,\, t) - l^{*2}Q_0^2\rho^{-2}\left(1 - \frac{2L_0}{\rho}\right)u_1(\rho,\, t) - \Omega^{-2}\frac{\partial^2}{\partial t^2}u_1(\rho,\, t) = 0. \tag{70}$$

To solve this equation, we will first use the method of separation of variables. Later, this restriction will be removed. Let

$$u_1(\rho,\ t) = u(\rho)\,T(t). \tag{71}$$

Substituting (71) into (70) and dividing by $u(\rho)T(t)$ yields the two ordinary differential equations

$$\frac{\mathrm{d}^2u(\rho)}{\mathrm{d}\rho^{*2}} - l^{*2}Q_0^2\rho^{-2}\left(1-\frac{2L_0}{\rho}\right)u(\rho) + \beta u(\rho) = 0, \tag{72}$$

$$\frac{\mathrm{d}^2T(t)}{\mathrm{d}t^2} + \beta\,\Omega^2T(t) = 0, \tag{73}$$

where $-\beta$ is the separation constant. The solution to (73) is

$$T(t) = c_3\sin(\omega t + c_4), \qquad c_3, c_4 \text{ constants}, \tag{74}$$

where we have chosen $\beta \equiv \omega^2/\Omega^2$, $\omega \ll \Omega$. Making this choice for β satisfies the requirement of (58) for a meaningful time average.

In order to solve equation (72), it is necessary to apply the high angular momentum approximation. It is therefore necessary to transform $C(\rho,\ t)$ to the x coordinate system and expand in inverse powers of $l^{*1/3}$ as is done for the unperturbed system [1]. The transformation in [1] for the unperturbed functions is repeated here for convenience

$$x = \left(\rho^* - l^*\right)l^{*-1/3}, \tag{75}$$

$$\begin{aligned}
\mathrm{d}\rho^* &\equiv l^{*1/3}\,\mathrm{d}x,\\
\rho &= l^* + l^{*1/3}r_0(x) + \cdots,\\
L_0 &= l^*\lambda_0(x) + l^{*2/3}\lambda_1(x) + l^{*1/3}\lambda_2(x) + \cdots,\\
Q_0 &= 1/k(x) + l^{*-1/3}q_1(x) + l^{*-2/3}q_2(x) + \cdots,\\
f_0 &= l^{*1/3}\phi(x) + \phi_1(x) + l^{*-1/3}\phi_2(x) + \cdots.
\end{aligned} \tag{76}$$

In addition, the function $u(\rho)$ must be expanded in a similar manner, i.e.

$$u = l^{*1/3}\mu_0(x) + \mu_1(x) + l^{*-1/3}\mu_2(x) + \cdots. \tag{77}$$

After a lengthy computation, the asymptotic expansion of (72) yields

$$l^{*1/3}\left(\frac{\omega^2}{\Omega^2} - \frac{1-2\lambda_0(x)}{k^2(x)}\right)\mu_0(x) + \mathrm{O}(1) = 0. \tag{78}$$

In order for (78) to be satisfied for large arbitrary l^* (in the limit $l^* \to \infty$), each order of $l^{*1/3}$ must be set to zero. Since setting $\mu_0(x) = 0$ implies the absence of electromagnetic wave perturbations, the bracketed term must be zero. It is known from the unperturbed system that [1]

$$\lambda_0(x) = \tfrac{1}{2}\left(1-k^2(x)\right). \tag{79}$$

Substituting (79) into (78) and setting the bracketed term to zero yields the relation

$$\omega^2 = \Omega^2 \tag{80}$$

which must hold in order to satisfy the condition $C(\rho, t) = 0$. However, equation (80) is a *contradiction* to the original assumption $\omega \ll \Omega$. Because of the presence of the contradiction, it is not necessary to solve the remaining field equations.

We arrived at this contradiction through the assumption that (70) could be solved by separating variables (equation (71)). The same result is obtained if $u_1(\rho,\ t)$ is not separable as is shown below. Modifying (77) as follows

$$u_1 = l^{*1/3}\mu_0(x,\ t) + \mu_1(x,\ t) + l^{*-1/3}\mu_2(x,\ t) + \cdots \tag{81}$$

and expanding (70) in inverse powers of $l^{*1/3}$ yields

$$-l^{*1/3}\left(\Omega^{-2}\frac{\partial^2}{\partial t^2}\mu_0(x,\ t) - \frac{1-2\lambda_0(x)}{k^2(x)}\right)\mu_0(x,\ t) + \mathrm{O}(1) = 0 \tag{82}$$

to lowest order in $l^{*1/3}$. Setting each order in $l^{*1/3}$ to zero requires $\mu_0(x,\ t)$ to satisfy the differential equation (using (79))

$$\frac{\partial^2}{\partial t^2}\mu_0(x,\ t) + \Omega^2\mu_0(x,\ t) = 0. \tag{83}$$

The solution is

$$\mu_0(x,\ t) = c_5(x)\sin(\Omega t + c_6(x)). \tag{84}$$

The characteristic frequency of $\mu_0(x,\ t)$ is Ω which contradicts the assumption $u_1(\rho,\ t) \sim \mu_0(x,\ t) \sim \omega \ll \Omega$.

Before we proceed with the discussion of the perturbation analysis based on (54)–(56), a second form for the wavefunction perturbation should be considered. Consider the perturbation in the form

$$\kappa_l\,\Omega\, a(\rho,\ t) = (f_0(\rho) + \delta u_1(\rho,\ t))\sin\Omega t + \mathrm{O}\left(\delta^2\right), \tag{85}$$

where the characteristic frequency of $u_1(\rho,\ t)$ is of order $\omega \ll \Omega$. This form can be interpreted as a slowly evolving amplitude of the rapidly varying function $\sin\Omega t$. Equations (54) and (85), in addition to the assumptions placed on $u_1(\rho,\ t)$, cover the entire range of possibilities for these types of perturbations (for example, a perturbation of the form $a(\rho,\ t) \to a(\rho + \delta\xi(\rho,\ t),\ t)$ reduces to (85)). Evaluation of the time averages yields

$$\kappa_l^2\,\Omega^2\left\langle a^2(\rho,\ t)\right\rangle_{\mathrm{T}} = \tfrac{1}{2}f_0^2 + \delta f_0 u_1 + \mathrm{O}\left(\delta^2\right), \tag{86}$$

$$\kappa_l^2\,\Omega^2\left\langle\left(\frac{\partial a}{\partial\rho^*}\right)^2\right\rangle_{\mathrm{T}} = \frac{1}{2}\left(\frac{\mathrm{d}f_0}{\mathrm{d}\rho^*}\right)^2 + \delta\frac{\mathrm{d}f_0}{\mathrm{d}\rho^*}\frac{\partial u_1}{\partial\rho^*} + \mathrm{O}\left(\delta^2\right), \tag{87}$$

$$\kappa_l^2\,\Omega^2\left\langle\left(\frac{\partial a}{\partial t}\right)^2\right\rangle_{\mathrm{T}} = \tfrac{1}{2}\Omega^2 f_0^2 + \delta\,\Omega^2 f_0 u_1 + \mathrm{O}\left(\delta^2\right), \tag{88}$$

$$\kappa_l^2\,\Omega^2\left\langle\frac{\partial a}{\partial t}\frac{\partial a}{\partial\rho^*}\right\rangle_{\mathrm{T}} = \delta\frac{1}{2}\frac{\mathrm{d}f_0}{\mathrm{d}\rho^*}\frac{\partial u_1}{\partial t} + \mathrm{O}\left(\delta^2\right). \tag{89}$$

Hence, the time dependence of the time-averaged functions becomes manifest at the first order in δ. This greatly increases the mathematical complexity of the system. The detailed analysis for this system is derived in appendix B for the case of $u_1(\rho,\ t)$ separable. From this analysis, the same contradiction results for the characteristic frequency of $u_1(\rho,\ t)$ as that found from the analysis based upon equation (54). For non-separable $u_1(\rho,\ t)$, the differential equations become unmanageable. Hence, it was not possible to obtain a conclusive result. However, due to the similar nature of the systems based upon equations (54) and (85), there is no reason to suspect a different result for the non-separable case.

4. Discussion

We have seen from the analysis of the static solution (section 2) that the confinement of geon constructs demands an absolutely critical choice of initial condition (amplitude eigenvalue). The slightest deviation from that choice leads to a totally unconfined structure. While some might argue that the confined structure being indicated with the critical initial condition is already satisfactory [6], the general experience with solitonic structures is one of essentially confined solutions in the neighbourhood of the best choice of critical condition [12]. The failure to find a family of near confinement in the case of the geon already raises suspicions as to its viability.

In the previous section, the time evolution of an electromagnetic geon equilibrium solution was studied with the objective of determining the time-scale of collapse away from the equilibrium configuration. Perturbations of the form (54) and (85) were analysed under certain assumptions. The problem of time averaging the source terms (right-hand side) of the field equations (45)–(47) requires the characteristic frequency ω of the perturbation term of the wavefunction $u_1(\rho,\ t)$ to be much less than the characteristic frequency Ω of the unperturbed solution. Without this assumption, the time dependence of the perturbations is lost upon time averaging, to all orders in the expansion. Hence, the assumption $u_1(\rho,\ t) \sim \omega \sim \Omega$ is not satisfactory for studying the time evolution of geons.

The assumption $u_1(\rho,\ t) \sim \omega \ll \Omega$, for both forms of the perturbation, solves the time-averaging problem in a simple manner. With this assumption, the differential equations maintain a time dependence after the time average has been taken over the typical period of the high-frequency waves. The perturbation analysis leads to the requirement $\omega \sim \Omega$ in order for the field equations to be satisfied. This is a contradiction to the original assumption $\omega \ll \Omega$. Since all the possible combinations for the form of the perturbation (and assumptions placed on $u_1(\rho,\ t)$) have been explored, the possible interpretations of the results of section 3 are given below.

A reasonable interpretation of the contradiction in the time-evolution analysis is that the condition of slow evolution of the background cannot be satisfied. Since not all of the required conditions are satisfied, it is not possible to construct a geon comprised of high-frequency waves. It could be argued that an electromagnetic geon could be built from low-frequency waves. This has not been ruled out by our model since it only accommodates high-frequency waves. However, a gravitational geon necessarily must be constructed from high-frequency waves, since otherwise the effective stress–energy would not be of the correct order of magnitude to create the background gravitational field binding the waves [3–5, 13]. Therefore, the gravitational geon studied in this paper is subject to the same fate as its high-frequency electromagnetic counterpart.

A geon with a rapidly evolving background metric, where the background is somehow regarded as being distinct from the small-amplitude waves on the background, is conceptually unsound. The definition presented in section 1 for this type of geon requires the background solution of the Einstein or Einstein–Maxwell field equations be quasi-stable on a time-scale much longer than the period of the constituent waves. If the background metric evolves away from the equilibrium configuration on the same time-scale as the constituent waves, one cannot speak of the waves binding gravitationally. Under these circumstances, there is no geon structure to identify. Further arguments against a rapidly evolving background metric can be found in [5].

The contradiction which arises in the perturbation analysis of section 3 is interpreted as a breakdown of the model, i.e. the perturbation model is not able to describe the evolution of the physical system. It might be argued that an alternative method of implementing the time evolution (not using perturbative methods) may be better suited to determine the time-scale of evolution. For example, it may be possible to develop an exact numerical solution of the full Einstein (or Einstein–Maxwell) equations without the splitting of the metric into a background and waves on the background or taking time averages. Considering the complexity involved in analysing the simple perturbative model of section 3, any new model would undoubtedly be more complex to solve. However, it should be possible to approximate any exact method with an appropriate perturbation expansion (as presented in section 3). Therefore, it is appropriate to consider the contradiction in a physical context, as was discussed earlier.

At this point, we recall the original motivation, which led the authors to re-open the issue of geons and their viability. One of the authors [14–16] had been led to propose a new hypothesis regarding the localization of energy in general relativity, namely that the energy was localized in regions of non-vanishing energy–momentum tensor $T^{\mu\nu}$. There were various factors leading to this. First, the energy–momentum conservation laws

$$T^{\mu\nu}{}_{;\nu} = 0 \tag{90}$$

are devoid of content in vacuum, producing the empty identity $0 = 0$. However, when (90) is re-expressed as a vanishing ordinary divergence to create a global form of the conservation law involving the introduction of pseudotensors, it is used to compute supposed fluxes of gravitational field energy in vacuum where the originating law is devoid of content. It was proposed that the ambiguity of the pseudotensorial flux vectors actually reflects the illegitimate injection of supposed physical content where none actually exists. Furthermore, it was shown that for Kerr–Schild metrics, all components of the gravitational pseudotensors vanish [17] and gravitational plane waves can be expressed in Kerr–Schild form. Since a wave is plane in a relatively small region, this is further support to the belief that waves of gravity are not actually carriers of energy in vacuum, in accord with the localization hypothesis. Other aspects to support the hypothesis had been outlined including the relationship to the important earlier papers of Nissani and Leibowitz [18], the basis for non-excitation of a Feynman detector and the work of Virbhadra [19] which showed that localization of energy is confined to the $T^{\mu\nu}$ regions for static and stationary spacetimes. The gravitational geon remained an outstanding challenge to the localization hypothesis since a purely gravitational non-singular construct displaying an unambiguous mass would be a clear counter-example. The present work adds new support for the hypothesis apart from the value of understanding this basic construct. From another viewpoint, the results which we have found in this paper are not surprising. From studies extending over 65 years, it was recognized that non-singular soliton structures to model elementary particles are not easily achieved and they are successful only with a careful mixture of different types of fields (see [12] for a review with earlier references contained therein). The electromagnetic geon depends only on the electromagnetic field and its own gravity, while the gravitational geon is even more restrictive, being a purely gravitational construct. In the light of earlier studies, it is not surprising that such simple ingredients should resist compactification.

5. Conclusions

The construction of a satisfactory gravitational geon model requires an asymptotically flat, self-consistent solution of the Einstein field equations, which meets the regularity conditions for a singularity-free spacetime. Furthermore, it must be demonstrated that the evolution in time of the geon must take place on a time-scale much longer than the characteristic period of the constituent waves (quasi-stability property).

To satisfy these conditions, it was proposed [3–5] that a satisfactory gravitational geon model must be constructed in a manner similar to that of Wheeler's [1] electromagnetic geon. This type of model for the gravitational geon is in contrast to the thin-shell model of Brill and Hartle [2]. In order to construct a gravitational geon in principle, it was previously established [3–5, 13] that gravitational waves of high frequency were necessary. The application of the high-frequency approximation reduced the gravitational and electromagnetic geon problem to the same set of ordinary differential equations and boundary conditions. Since the background metric is initially assumed to be static, any solutions are necessarily equilibrium solutions. From a phase portrait analysis of the ordinary differential equations governing gravitational and electromagnetic geons, it was possible to determine both the existence and stability properties of equilibrium solutions with respect to perturbations of the amplitude eigenvalues. It was found that admissible equilibrium solutions were unstable to changes in the amplitude eigenvalues. Since a basic requirement for the existence of both types of geon is the quasi-stability property, an investigation of the time evolution of an electromagnetic geon was performed. In contrast to other investigations, a small-amplitude time-dependent perturbation to an equilibrium solution was applied. The time-averaging problem is solved by assuming the characteristic frequency of the perturbations vary on a time-scale which is much longer than that of the waves comprising the electromagnetic geon. This is in accordance with the requirement that the background metric be quasi-stable. Solving the time-dependent perturbation equations leads to the characteristic frequency of the perturbations being of the same order in magnitude as the waves comprising the electromagnetic geon. This is a contradiction to the original assumption. Thus it could not be shown that the time evolution of the electromagnetic geon proceeds on a slow time-scale using standard perturbation theory modified for time-averaged fields. With not all of the requirements for the existence of an electromagnetic geon being satisfied, it cannot be concluded that an electromagnetic or a gravitational geon is a viable entity.

Given the results as applied to the gravitational geon, such a construct cannot be considered a counter-example to the energy localization hypothesis as discussed in [14–16].

Acknowledgments

The authors would like to thank Dr S Bohun for helpful discussions. This research was supported, in part, by a grant from the Natural Sciences and Engineering Research Council of Canada and a Natural Sciences and Engineering Research Council Postgraduate Scholarship (GPP).

Appendix A. Time-dependent electromagnetic geon equations

We start by defining the electromagnetic vector potential for one mode of the electromagnetic waves

$$A_\mu = \big(0,\ 0,\ 0,\ A_\varphi\big), \tag{A1}$$

where

$$A_\varphi = a(r,t)B_l(\theta), \qquad B_l(\theta) = \sin\theta \frac{\mathrm{d}}{\mathrm{d}\theta} P_l(\cos\theta). \tag{A2}$$

The time-dependent metric is

$$\mathrm{d}s^2 = g_{\alpha\beta}\,\mathrm{d}x^\alpha\,\mathrm{d}x^\beta = -\mathrm{e}^\nu\,\mathrm{d}t^2 + \mathrm{e}^\lambda\,\mathrm{d}r^2 + r^2\,\mathrm{d}\theta^2 + r^2\sin^2\theta\,\mathrm{d}\varphi^2, \tag{A3}$$

where

$$\nu = \nu(r, t), \qquad \lambda = \lambda(r, t).$$

In the absence of charges and currents, Maxwell's equations in a curved spacetime are

$$\frac{1}{\sqrt{-g}} \frac{\partial}{\partial x^\alpha} \left(\sqrt{-g} F^{\beta\alpha} \right) = 0, \tag{A4}$$

$$F_{\alpha\beta,\gamma} + F_{\gamma\alpha,\beta} + F_{\beta\gamma,\alpha} = 0, \tag{A5}$$

where g is the determinant of the metric (A3) and the Maxwell tensor, $F_{\alpha\beta}$, is related to the 4-vector potential as $F_{\alpha\beta} = A_{\beta,\alpha} - A_{\alpha,\beta}$. The only non-trivial equation is for $\alpha = \varphi$ in (A4). It yields the wave equation

$$\frac{\partial^2 a}{\partial r^{*2}} - \frac{l(l+1)}{r^2} \mathrm{e}^{\nu} a - \mathrm{e}^{\nu-\lambda} \frac{\partial^2 a}{\partial t^{*2}} = 0, \tag{A6}$$

where

$$\frac{\partial}{\partial r^*} = \mathrm{e}^{(\nu-\lambda)/2} \frac{\partial}{\partial r}, \qquad \frac{\partial^2}{\partial r^{*2}} = \mathrm{e}^{(\nu-\lambda)/2} \frac{\partial}{\partial r} \left(\mathrm{e}^{(\nu-\lambda)/2} \frac{\partial}{\partial r} \right), \tag{A7}$$

$$\frac{\partial}{\partial t^*} = \mathrm{e}^{(\nu-\lambda)/2} \frac{\partial}{\partial t}, \qquad \frac{\partial^2}{\partial t^{*2}} = \mathrm{e}^{(\nu-\lambda)/2} \frac{\partial}{\partial t} \left(\mathrm{e}^{(\nu-\lambda)/2} \frac{\partial}{\partial t} \right). \tag{A8}$$

The Einstein equations for the electromagnetic geon are

$$G_\mu{}^\nu = 8\pi \left\langle T_\mu{}^\nu \right\rangle, \tag{A9}$$

where $\langle\cdot\rangle$ denotes a time–space average over all N active modes of the electromagnetic waves. In the equations below, the energy–momentum tensor for a single mode of electromagnetic radiation is given by

$$T_{(\mathrm{I})\,\mu}{}^\nu \equiv \frac{1}{4\pi} \left(F_{\mu\sigma} F^{\sigma\nu} - \tfrac{1}{4} F_{\alpha\beta} F^{\alpha\beta} \delta^\nu_\mu \right), \tag{A10}$$

with $F_{\alpha\beta}$ defined above. We will only evaluate the angle average of $T_\mu{}^\nu$. The time average will be dealt with in the main text (section 3). In addition to the three angle averages [1]†

$$\left\langle T_t{}^t \right\rangle_{\mathrm{TA}} = \tfrac{1}{2} N \int_0^\pi \left\langle T_{(\mathrm{I})\,t}{}^t \right\rangle_{\mathrm{T}} \sin\theta \, \mathrm{d}\theta, \tag{A11}$$

$$\left\langle T_r{}^r \right\rangle_{\mathrm{TA}} = \tfrac{1}{2} N \int_0^\pi \left\langle T_{(\mathrm{I})\,r}{}^r \right\rangle_{\mathrm{T}} \sin\theta \, \mathrm{d}\theta, \tag{A12}$$

$$\left\langle T_\theta{}^\theta \right\rangle_{\mathrm{TA}} = \left\langle T_\varphi{}^\varphi \right\rangle_{\mathrm{TA}} = \tfrac{1}{2} N \int_0^\pi \left\langle T_{(\mathrm{I})\,\theta}{}^\theta + T_{(\mathrm{I})\,\varphi}{}^\varphi \right\rangle_{\mathrm{T}} \sin\theta \, \mathrm{d}\theta, \tag{A13}$$

there is an additional average, which represents the radial flow of energy,

$$\left\langle T_r{}^t \right\rangle_{\mathrm{TA}} = \tfrac{1}{2} N \int_0^\pi \left\langle T_{(\mathrm{I})\,r}{}^t \right\rangle_{\mathrm{T}} \sin\theta \, \mathrm{d}\theta. \tag{A14}$$

Evaluating (A11)–(A14) using (A1) and the integrals of appendix C one obtains

$$\left\langle T_t{}^t \right\rangle_{\mathrm{TA}} = -\frac{N l(l+1)}{8\pi r^2 (2l+1)} \left(\mathrm{e}^{-\nu} \left\langle a_{,t}^2 \right\rangle_{\mathrm{T}} + \mathrm{e}^{-\lambda} \left\langle a_{,r}^2 \right\rangle_{\mathrm{T}} + \frac{l(l+1)}{r^2} \left\langle a^2 \right\rangle_{\mathrm{T}} \right), \tag{A15}$$

$$\left\langle T_r{}^r \right\rangle_{\mathrm{TA}} = \frac{N l(l+1)}{8\pi r^2 (2l+1)} \left(\mathrm{e}^{-\nu} \left\langle a_{,t}^2 \right\rangle_{\mathrm{T}} + \mathrm{e}^{-\lambda} \left\langle a_{,r}^2 \right\rangle_{\mathrm{T}} - \frac{l(l+1)}{r^2} \left\langle a^2 \right\rangle_{\mathrm{T}} \right), \tag{A16}$$

† The symbols $\langle\cdot\rangle_{\mathrm{TA}}$ and $\langle\cdot\rangle_{\mathrm{T}}$ denote a time–angle average and a time average, respectively.

$$\langle T_\theta{}^\theta\rangle_{\mathrm{TA}} = \frac{Nl^2(l+1)^2}{8\pi r^4(2l+1)}\langle a^2\rangle_{\mathrm{T}}, \tag{A17}$$

$$\langle T_r{}^t\rangle_{\mathrm{TA}} = -\frac{Nl(l+1)}{4\pi \mathrm{e}^\nu r^2(2l+1)}\langle a_{,r}a_{,t}\rangle_{\mathrm{T}}. \tag{A18}$$

The components of the left-hand side of (A9) are

$$G_t{}^t = -r^{-2} + r^{-2}\mathrm{e}^{-\lambda} - r^{-1}\mathrm{e}^{-\lambda}\lambda_{,r} \tag{A19}$$

$$G_r{}^r = -r^{-2} + r^{-2}\mathrm{e}^{-\lambda} + r^{-1}\mathrm{e}^{-\lambda}\nu_{,r} \tag{A20}$$

$$G_\theta{}^\theta = G_\varphi{}^\varphi = \tfrac{1}{2}\left(\mathrm{e}^{-\lambda}\left(r^{-1}\nu_{,r} - r^{-1}\lambda_{,r} + \nu_{,rr} - \tfrac{1}{2}\lambda_{,r}\nu_{,r} + \tfrac{1}{2}\nu_{,r}^2\right) + \mathrm{e}^{-\nu}\left(\tfrac{1}{2}\lambda_{,t}\nu_{,t} - \lambda_{,tt} - \tfrac{1}{2}\lambda_{,t}^2\right)\right) \tag{A21}$$

$$G_r{}^t = -r^{-1}\mathrm{e}^{-\nu}\lambda_{,t}. \tag{A22}$$

The final step in obtaining the time-dependent electromagnetic geon field equations is to make the transformation to the ρ coordinate system. In addition to the transformation

$$r = \frac{\rho}{\Omega}, \tag{A23}$$

we introduce the two metric functions $L(\rho,\ t)$ and $Q(\rho,\ t)$ through the defining equations

$$\mathrm{e}^{-\lambda} \equiv 1 - \frac{2L(\rho,\ t)}{\rho}, \tag{A24}$$

$$\mathrm{e}^{\lambda+\nu} \equiv Q^2(\rho,\ t), \tag{A25}$$

$$\mathrm{e}^{\nu} = \left(1 - \frac{2L(\rho,\ t)}{\rho}\right)Q^2(\rho,\ t). \tag{A26}$$

The operator $\partial/\partial r^*$ has the following form in the ρ coordinate system:

$$\frac{\partial}{\partial r^*} = \mathrm{e}^{(\nu-\lambda)/2}\frac{\partial}{\partial r} = \Omega\left(1 - \frac{2L}{\rho}\right)Q\frac{\partial}{\partial\rho}. \tag{A27}$$

By defining

$$\frac{\partial}{\partial\rho^*} \equiv \left(1 - \frac{2L}{\rho}\right)Q\frac{\partial}{\partial\rho}, \tag{A28}$$

the operators of (A7) simply transform as

$$\frac{\partial}{\partial r^*} = \Omega\frac{\partial}{\partial\rho^*}, \qquad \frac{\partial^2}{\partial r^{*2}} = \Omega^2\frac{\partial^2}{\partial\rho^{*2}}. \tag{A29}$$

The operator $\partial^2/\partial t^{*2}$ of (A8) transforms as

$$\frac{\partial^2}{\partial t^{*2}} = \left(1 - \frac{2L}{\rho}\right)^{-1}Q^{-1}\frac{\partial}{\partial t}\left(\left(1 - \frac{2L}{\rho}\right)^{-1}Q^{-1}\frac{\partial}{\partial t}\right). \tag{A30}$$

After applying the transformation (A23) and equations (A24)–(A30), a lengthy but straightforward computation yields the wave equation

$$\Omega^2\frac{\partial^2 a}{\partial\rho^{*2}} - \Omega^2 l^{*2}\rho^{-2}\left(1 - \frac{2L}{\rho}\right)Q^2 a - \left(1 - \frac{2L}{\rho}\right)^2 Q^2\frac{\partial^2 a}{\partial t^{*2}} = 0 \tag{A31}$$

and the background field equations

$$\frac{\partial L}{\partial \rho^*} = \frac{\kappa_l^2}{2}\left(Q^{-1}\left(\Omega^2\left\langle\left(\frac{\partial a}{\partial \rho^*}\right)^2\right\rangle_{\mathrm{T}} + \left\langle\left(\frac{\partial a}{\partial t}\right)^2\right\rangle_{\mathrm{T}}\right) + \Omega^2 l^{*2}\rho^{-2}\left(1-\frac{2L}{\rho}\right)Q\left\langle a^2\right\rangle_{\mathrm{T}}\right), \tag{A32}$$

$$\frac{\partial Q}{\partial \rho^*} = \frac{\kappa_l^2}{\rho - 2L}\left(\Omega^2\left\langle\left(\frac{\partial a}{\partial \rho^*}\right)^2\right\rangle_{\mathrm{T}} + \left\langle\left(\frac{\partial a}{\partial \rho^*}\right)^2\right\rangle_{\mathrm{T}}\right), \tag{A33}$$

$$\frac{\partial L}{\partial t} = \kappa_l^2\Omega^2 Q^{-1}\left\langle\frac{\partial a}{\partial \rho^*}\frac{\partial a}{\partial t}\right\rangle_{\mathrm{T}} \tag{A34}$$

and

$$\begin{aligned}\frac{\partial^2 L}{\partial t^2} + 4\rho^{-1}\left(\frac{\partial L}{\partial t}\right)^2 - Q^{-1}\frac{\partial L}{\partial t}\frac{\partial Q}{\partial t} &= \frac{1}{2}\left(1-\frac{2L}{\rho}\right)^2 Q^2\rho \\ &\quad\times\left(\mathcal{A}(\rho) + \mathcal{B}(\rho) - 2\kappa^2 l^{*2}\Omega^4\rho^{-4}\left\langle a^2\right\rangle_{\mathrm{T}}\right).\end{aligned} \tag{A35}$$

In the above equations we have defined

$$\kappa_l \equiv \sqrt{\frac{Nl^{*2}}{2l+1}} \qquad l^* \equiv \sqrt{l(l+1)}, \tag{A36}$$

$$\mathcal{A}(\rho) \equiv 2\Omega^2\rho^{-1}\left(Q^{-1}\frac{\partial Q}{\partial \rho}\left(1-\frac{2L}{\rho}\right) + 2\rho^{-1}\left(\rho^{-1}L - \frac{\partial L}{\partial \rho}\right)\right) \tag{A37}$$

and

$$\begin{aligned}\mathcal{B}(\rho) \equiv \Omega^2\left(1-\frac{2L}{\rho}\right)\Bigg(2\Bigg(&2Q^{-1}\left(\frac{\partial^2 Q}{\partial \rho^2} - Q^{-1}\left(\frac{\partial Q}{\partial \rho}\right)^2\right) \\ &-2\rho^{-2}\left(1-\frac{2L}{\rho}\right)^{-1}\left(\rho^{-1}L - \frac{\partial L}{\partial \rho}\right) \\ &+4\rho^{-2}\left(1-\frac{2L}{\rho}\right)^{-2}\left(\rho^{-1}L - \frac{\partial L}{\partial \rho}\right)^2 \\ &+2\rho^{-2}\left(1-\frac{2L}{\rho}\right)^{-1}\left(\frac{\partial L}{\partial \rho} - \rho^{-1}L - \rho\frac{\partial^2 L}{\partial \rho^2}\right)\Bigg) \\ &-\left(2\rho^{-1}\left(1-\frac{2L}{\rho}\right)^{-1}\left(\frac{\partial L}{\partial \rho} - \rho^{-1}L\right)\right) \\ &\times\left(2Q^{-1}\frac{\partial Q}{\partial \rho} - 2\rho^{-1}\left(1-\frac{2L}{\rho}\right)^{-1}\left(\frac{\partial L}{\partial \rho} - \rho^{-1}L\right)\right) \\ &+\left(2Q^{-1}\frac{\partial Q}{\partial \rho} - 2\rho^{-1}\left(1-\frac{2L}{\rho}\right)^{-1}\left(\frac{\partial L}{\partial \rho} - \rho^{-1}L\right)\right)^2\Bigg).\end{aligned} \tag{A38}$$

Equations (A31)–(A34) are equations (44)–(47) of section 3.

Appendix B. Perturbation analysis of a slowly varying amplitude

To investigate the time evolution of the unperturbed solution, the equilibrium solution (51)–(53) will be perturbed by allowing the coefficient of $\sin\Omega t$ to become a slowly varying function of time as compared to the period $2\pi\Omega^{-1}$ of the electromagnetic waves. In addition, it will be assumed that $u_1(\rho, t)$ is a separable function (i.e. $u_1(\rho, t) = u(\rho)T(t)$). Under this assumption, equation (85) becomes

$$\kappa_l\,\Omega\,a(\rho, t) = (f_0(\rho) + \delta u(\rho)T(t))\sin\Omega t, \tag{B1}$$

where the characteristic frequency of $u(\rho)T(t)$ is of order $\omega \ll \Omega$. This introduces a small time-dependent perturbation in the metric functions

$$L(\rho, t) = L_0(\rho) + \delta L_1(\rho, t), \tag{B2}$$

$$Q(\rho, t) = Q_0(\rho) + \delta Q_1(\rho, t). \tag{B3}$$

It is stated without proof that for $u_1(\rho, t)$ separable, the field equations impose the relations $u(\rho) = f_0(\rho)$ and $T(t) = \sin(\omega t)$. Therefore, the analysis in this appendix is carried out for the perturbation

$$\kappa_l\,\Omega\,a(\rho, t) = (f_0(\rho) + \delta f_0(\rho)\sin\omega t)\sin\Omega t, \qquad \omega \ll \Omega, \quad \delta \ll 1. \tag{B4}$$

The perturbation expansion will be taken to the first order in δ. We have assumed that the coefficient $f(\rho, t) \equiv f_0(\rho) + \delta f_0(\rho)\sin\omega t$ of $\sin\Omega t$ in (B4) varies on a time-scale much longer than that of $\sin\Omega t$. Therefore, $f(\rho, t)$ is approximately constant over the short time period $T = 2\pi\Omega^{-1}$ of the electromagnetic waves. Therefore, evaluation of the time averages (86)–(89) yields

$$\kappa_l^2\,\Omega^2\left\langle a^2(\rho, t)\right\rangle_{\mathrm{T}} = \tfrac{1}{2} f_0^2\,(1 + 2\delta\sin\omega t) + \mathrm{O}\left(\delta^2\right), \tag{B5}$$

$$\kappa_l^2\,\Omega^2\left\langle\left(\frac{\partial a}{\partial\rho^*}\right)^2\right\rangle_{\mathrm{T}} = \frac{1}{2}\left(\frac{\mathrm{d}f_0}{\mathrm{d}\rho^*}\right)^2(1 + 2\delta\sin\omega t) + \mathrm{O}\left(\delta^2\right), \tag{B6}$$

$$\kappa_l^2\,\Omega^2\left\langle\left(\frac{\partial a}{\partial t}\right)^2\right\rangle_{\mathrm{T}} = \tfrac{1}{2}\Omega^2 f_0^2\,(1 + 2\delta\sin\omega t) + \mathrm{O}\left(\delta^2\right), \tag{B7}$$

$$\kappa_l^2\,\Omega^2\left\langle\frac{\partial a}{\partial t}\frac{\partial a}{\partial\rho^*}\right\rangle_{\mathrm{T}} = \tfrac{1}{2}\delta\omega f_0\frac{\mathrm{d}f_0}{\mathrm{d}\rho^*}\cos\omega t + \mathrm{O}\left(\delta^2\right). \tag{B8}$$

Substitution of (B4)–(B8) into (44)–(47), expanding to first order in δ and setting each order to zero yields the unperturbed equations (63)–(65) and the first-order equations (B9)–(B14). Setting the first-order part of the wave equation (44) to zero yields

$$A(\rho, t)\sin\Omega t + B(\rho, t)\cos\Omega t = 0, \tag{B9}$$

where

$$\begin{aligned} A(\rho, t) \equiv \Omega^2\Bigg(&\omega^2\Omega^{-2} f_0 + \left(1 - l^{*2}\rho^{-2}Q_0^2\left(1 - \frac{2L_0}{\rho}\right)\right) f_0 + Q_0\left(1 - \frac{2L_0}{\rho}\right)\\ &\times\Bigg(2\rho^{-2}Q_0\frac{\mathrm{d}f_0}{\mathrm{d}\rho}\left(L_0 - \rho\frac{\mathrm{d}L_0}{\mathrm{d}\rho}\right) + Q_0\frac{\mathrm{d}^2 f_0}{\mathrm{d}\rho^2}\left(1 - \frac{2L_0}{\rho}\right)\\ &+\frac{\mathrm{d}f_0}{\mathrm{d}\rho}\frac{\mathrm{d}Q_0}{\mathrm{d}\rho}\left(1 - \frac{2L_0}{\rho}\right)\Bigg)\Bigg)\sin\omega t + \Omega^2\Bigg(Q_0\left(1 - \frac{2L_0}{\rho}\right)\\ &\times\Bigg(2\rho^{-2}\frac{\mathrm{d}f_0}{\mathrm{d}\rho}\left(Q_1\left(L_0 - \rho\frac{\mathrm{d}L_0}{\mathrm{d}\rho}\right) + Q_0\left(L_1(\rho, t) - \rho\frac{\partial}{\partial\rho}L_1(\rho, t)\right)\right)\\ &+\left(\left(1 - \frac{2L_0}{\rho}\right)\frac{\partial}{\partial\rho}Q_1(\rho, t) - 2\rho^{-1}L_1(\rho, t)\frac{\mathrm{d}Q_0}{\mathrm{d}\rho}\right)\frac{\mathrm{d}f_0}{\mathrm{d}\rho}\end{aligned}$$

$$+\left(Q_1(\rho,\ t)\left(1-\frac{2L_0}{\rho}\right)-2\rho^{-1}L_1(\rho,\ t)Q_0\right)\frac{\mathrm{d}^2 f_0}{\mathrm{d}\rho^2}\Bigg)$$
$$+2\rho^{-3}\left(l^{*2}Q_0^2L_1(\rho,\ t)-l^{*2}\rho Q_0Q_1(\rho,\ t)\left(1-\frac{2L_0}{\rho}\right)\right)f_0$$
$$+\left(Q_1(\rho,\ t)\left(1-\frac{2L_0}{\rho}\right)-2\rho^{-1}L_1(\rho,\ t)Q_0\right)\left(2\rho^{-2}\frac{\mathrm{d}f_0}{\mathrm{d}\rho}Q_0\left(L_0-\rho\frac{\mathrm{d}L_0}{\mathrm{d}\rho}\right)\right.$$
$$\left.+\left(1-\frac{2L_0}{\rho}\right)\left(Q_0\frac{\mathrm{d}^2 f_0}{\mathrm{d}\rho^2}+\frac{\mathrm{d}Q_0}{\mathrm{d}\rho}\frac{\mathrm{d}f_0}{\mathrm{d}\rho}\right)\right)\Bigg) \tag{B10}$$

and

$$B(\rho,\ t)\equiv\Omega f_0\left(2\rho^{-1}\left(1-\frac{2L}{\rho}\right)^{-1}\frac{\partial}{\partial t}L_1(\rho,\ t)-Q_0^{-1}\frac{\partial}{\partial t}Q_1(\rho,\ t)+2\omega\cos\omega t\right). \tag{B11}$$

The derivatives of $L_1(\rho,\ t)$ and $Q_1(\rho,\ t)$ with respect to ρ are found from the first-order equations

$$\left(1-\frac{2L_0}{\rho}\right)Q_0\frac{\partial}{\partial\rho}L_1(\rho,\ t)=-\left(\left(1-\frac{2L_0}{\rho}\right)Q_1(\rho,\ t)-2\rho^{-1}L_1(\rho,\ t)Q_0\right)\frac{\mathrm{d}L_0}{\mathrm{d}\rho}$$
$$+\tfrac{1}{2}Q_0^{-1}\left(Q_0^2\left(1-\frac{2L_0}{\rho}\right)^2\left(\frac{\mathrm{d}f_0}{\mathrm{d}\rho}\right)^2\sin\omega t+\left(\left(1-\frac{2L_0}{\rho}\right)^2Q_0Q_1(\rho,\ t)\right.\right.$$
$$\left.-2\rho^{-1}Q_0^2\left(1-\frac{2L_0}{\rho}\right)L_1(\rho,\ t)\right)\left(\frac{\mathrm{d}f_0}{\mathrm{d}\rho}\right)^2+f_0^2\sin^2\omega t\Bigg)$$
$$-\frac{1}{2}Q_0^{-2}Q_1(\rho,\ t)\left(\frac{1}{2}\left(1-\frac{2L_0}{\rho}\right)^2Q_0^2\left(\frac{\mathrm{d}f_0}{\mathrm{d}\rho}\right)^2+\frac{1}{2}f_0^2\right)$$
$$+\tfrac{1}{2}l^{*2}\rho^{-2}Q_0f_0^2\left(1-\frac{2L_0}{\rho}\right)\sin\omega t$$
$$+\tfrac{1}{4}\left(l^{*2}\rho^{-2}\left(1-\frac{2L_0}{\rho}\right)Q_1(\rho,\ t)-2l^{*2}\rho^{-3}L_1(\rho,\ t)Q_0\right)f_0^2 \tag{B12}$$

and

$$\left(1-\frac{2L_0}{\rho}\right)Q_0\frac{\partial}{\partial\rho}Q_1(\rho,\ t)=-\left(\left(1-\frac{2L_0}{\rho}\right)Q_1(\rho,\ t)-2\rho^{-1}L_1(\rho,\ t)Q_0\right)\frac{\mathrm{d}Q_0}{\mathrm{d}\rho}$$
$$+\frac{1}{\rho-2L_0}\left(\left(1-\frac{2L_0}{\rho}\right)^2Q_0^2\left(\frac{\mathrm{d}f_0}{\mathrm{d}\rho}\right)^2\sin\omega t\right.$$
$$+\frac{1}{2}\left(2\left(1-\frac{2L_0}{\rho}\right)^2Q_0Q_1(\rho,\ t)\right.$$
$$\left.\left.-4\rho^{-1}\left(1-\frac{2L_0}{\rho}\right)L_1(\rho,\ t)Q_0^2\right)\left(\frac{\mathrm{d}f_0}{\mathrm{d}\rho}\right)^2+f_0^2\sin^2\omega t\right)$$
$$+\frac{L_1(\rho,\ t)}{(\rho-2L_0)^2}\left(\left(1-\frac{2L_0}{\rho}\right)^2Q_0^2\left(\frac{\mathrm{d}f_0}{\mathrm{d}\rho}\right)^2+f_0^2\right), \tag{B13}$$

respectively. The derivative of $L_1(\rho,\ t)$ with respect to t is given by the first-order equation

$$\frac{\partial}{\partial t}L_1(\rho,\ t)=\frac{1}{2}\omega\left(1-\frac{2L_0}{\rho}\right)f_0\frac{\mathrm{d}f_0}{\mathrm{d}\rho}\cos\omega t. \tag{B14}$$

The simplest of the first-order equations is (B14). It is immediately integrable to yield

$$L_1(\rho,\ t) = \frac{1}{2}\left(1 - \frac{2L_0}{\rho}\right) f_0 \frac{\mathrm{d}f_0}{\mathrm{d}\rho} \sin\omega t + c_1(\rho), \tag{B15}$$

where $c_1(\rho)$ is a function of ρ. It is possible to obtain an equation for $\partial Q_1(\rho,\ t)/\partial t$ from (B9). This is done by substituting (B14) into the coefficient of $\cos\Omega t$ (namely $B(\rho,\ t)$) and setting the expression to zero. This is justified since $\sin\Omega t$ and $\cos\Omega t$ are independent functions in the approximation that $A(\rho,\ t)$ and $B(\rho,\ t)$ are slowly varying functions of time. Solving for $\partial Q_1(\rho,\ t)/\partial t$ and integrating yields

$$Q_1(\rho,\ t) = Q_0\left(2 + \rho^{-1} f_0 \frac{\mathrm{d}f_0}{\mathrm{d}\rho}\right)\sin\omega t + c_2(\rho). \tag{B16}$$

Up to this point the only first-order field equation which has been satisfied is (B14). To satisfy the first-order wave equation (B9), the condition $A(\rho,\ t) = 0$ must be imposed. By using the first-order field equations (B12) and (B13), the ρ derivatives of $L_1(\rho,\ t)$ and $Q_1(\rho,\ t)$ found in $A(\rho,\ t)$ (equation (B10)) can be eliminated. After substitution of (B15) and (B16) into (B10), $A(\rho,\ t)$ no longer depends on the first-order functions $L_1(\rho,\ t)$ and $Q_1(\rho,\ t)$. As a result of these substitutions, (B10) takes the form†

$$\mathcal{A}(\rho)\sin\omega t + \mathcal{B}(c_1(\rho),\ c_2(\rho),\ \rho) = 0, \tag{B17}$$

where $\mathcal{A}(\rho)$ and $\mathcal{B}(\rho)$ depend only on ρ, the unperturbed functions $f_0(\rho)$, $L_0(\rho)$, $Q_0(\rho)$ (and their derivatives) and the two functions $c_1(\rho)$ and $c_2(\rho)$. Note that $c_1(\rho)$ and $c_2(\rho)$ are only found in $\mathcal{B}(\rho)$. Equation (B17) will be satisfied for all t only if $\mathcal{A}(\rho) = 0$ and $\mathcal{B}(\rho) = 0$. Since $c_1(\rho)$ and $c_2(\rho)$ are yet to be determined, we will focus upon the equation $\mathcal{A}(\rho) = 0$.

The function $\mathcal{A}(\rho)$ is comprised of the known functions $f_0(\rho)$, $L_0(\rho)$ and $Q_0(\rho)$. It is therefore necessary to transform $\mathcal{A}(\rho)$ to the x coordinate system and expand in inverse powers of $l^{*1/3}$ as is done for the unperturbed system [1]. The transformation is given by equations (75)–(76). After a lengthy computation, the asymptotic expansion of $\mathcal{A}(\rho) = 0$ yields

$$l^{*1/3}\left(k^{-2}(x)\left(10\lambda_0(x) - 5 + k^2(x)\right) + \frac{\omega^2}{\Omega^2}\right)\phi(x) + \mathrm{O}(1) = 0. \tag{B18}$$

In order for (B18) to be satisfied for large arbitrary l^* (in the limit $l^* \to \infty$), each order of $l^{*1/3}$ must be set to zero. Since setting $\phi(x) = 0$ implies the absence of electromagnetic wave perturbations, the bracketed term must be zero. It is known from the unperturbed system that [1]

$$\lambda_0(x) = \tfrac{1}{2}\left(1 - k^2(x)\right). \tag{B19}$$

Substitution of (B19) in (B18) leads to the relation

$$\omega^2 = 4\Omega^2 \tag{B20}$$

which must hold in order for the field equation (B9) to be satisfied. However, equation (B20) is a *contradiction* to the original assumption $\omega \ll \Omega$. This result is identical to that found for the perturbation analysis based upon equation (54).

† Explicit forms of $\mathcal{A}(\rho)$ and $\mathcal{B}(\rho)$ will not be given due to their extreme length.

Appendix C. Angle average of T_μ^ν

Equations (A11)–(A14) include integrating over the angle φ and dividing by the solid angle 4π, thus all that is left is evaluating the θ integrals. The θ dependence of $T_\mu{}^\nu$ comes in three forms

$$\sin^{-2}\theta\,(\Theta_l(\theta))^2\,, \qquad \sin^{-2}\theta\left(\Theta_l(\theta)_{,\theta}\right)^2 \qquad \text{and} \qquad \sin^{-2}\theta\;\Theta_l(\theta)\Theta_l(\theta)_{,\theta\theta} \tag{C1}$$

where

$$\Theta_l(\theta) = C_l^0 B_l(\theta) \tag{C2}$$

and

$$B_l(\theta) \equiv \sin\theta\,\frac{\mathrm{d}}{\mathrm{d}\theta}\,P_l(\cos\theta). \tag{C3}$$

The exact integrals are evaluated below:

$$\int_0^\pi \sin^{-2}\theta\,(B_l(\theta))^2\sin\theta\,\mathrm{d}\theta = \frac{2l(l+1)}{2l+1}, \tag{C4}$$

$$\int_0^\pi \sin^{-2}\theta\left(B_l(\theta)_{,\theta}\right)^2\sin\theta\,\mathrm{d}\theta = \frac{2l^2(l+1)^2}{2l+1}, \tag{C5}$$

$$\int_0^\pi \sin^{-2}\theta\,B_l(\theta)B_l(\theta)_{,\theta\theta}\sin\theta\,\mathrm{d}\theta = -\frac{2l^3(l+1)}{2l+1}. \tag{C6}$$

The normalization constant for $\Theta_l(\theta)$ is found by requiring

$$\int_0^{2\pi}\int_0^\pi |\Theta_l(\theta)|^2\sin\theta\,\mathrm{d}\theta\,\mathrm{d}\varphi = 1. \tag{C7}$$

Therefore,

$$\left(C_l^0\right)^2 = \frac{1}{2\pi}\left(\int_0^\pi (B_l(\theta))^2\sin\theta\,\mathrm{d}\theta\right)^{-1} = \frac{1}{2\pi}\left(\frac{4l^2(l+1)^2}{(2l-1)(2l+1)(2l+3)}\right)^{-1}. \tag{C8}$$

Thus the normalization constant is

$$C_l^0 = \left(\frac{(2l-1)(2l+1)(2l+3)}{8\pi l^2(l+1)^2}\right)^{1/2}. \tag{C9}$$

References

[1] Wheeler J A 1955 *Phys. Rev.* **97** 511

[2] Brill D R and Hartle J B 1964 *Phys. Rev.* B **135** 271

[3] Cooperstock F I, Faraoni V and Perry G P 1995 *Mod. Phys. Lett.* A **10** 359

[4] Cooperstock F I, Faraoni V and Perry G P 1996 *Proc. 7th Marcel Grossmann Meeting on General Relativity* ed R T Jantzen and G MacKeiser (Singapore: World Scientific) p 351

[5] Cooperstock F I, Faraoni V and Perry G P 1996 *Int. J. Mod. Phys.* D **5** 375

[6] Anderson P R and Brill D R 1997 *Phys. Rev.* D **56** 4824

[7] Brill D R 1966 *Perspectives in Geometry and Relativity, Essays in Honor of Václav Hlavatý* ed B Hoffmann (Bloomington, IN: Indiana University Press) p 38

[8] Jordan D W and Smith P 1987 *Nonlinear Ordinary Differential Equations* (Oxford: Oxford University Press) 2nd edn

[9] Ernst F J 1957 *Phys. Rev.* **105** 1665

[10] Perry G P 1998 *PhD Thesis* University of Victoria

[11] Eisberg R and Resnick R 1985 *Quantum Physics of Atoms, Molecules, Solids, Nuclei, and Particles* 2nd edn (New York: Wiley) p 203

[12] Cooperstock F I and Rosen N 1989 *Int. J. Theor. Phys.* **28** 423
[13] Isaacson R A 1968 *Phys. Rev.* **166** 1263
Isaacson R A 1968 *Phys. Rev.* **166** 1272
[14] Cooperstock F I 1992 *Found. Phys.* **22** 1011
[15] Cooperstock F I 1993 *Topics in Quantum Gravity and Beyond* ed F Mansouri and J J Scanio (Singapore: World Scientific) p 201
[16] Cooperstock F I 1997 *Relativistic Astrophysics and Cosmology* ed J Buitrago, E Mediavilla and A Oscoz (Singapore: World Scientific) p 61
[17] Gürses M and Gürsey F 1975 *J. Math. Phys.* **16** 2385
[18] Nissani N and Leibowitz E 1988 *Phys. Lett.* A **126** 447
Nissani N and Leibowitz E 1989 *Int. J. Theor. Phys.* **28** 235
Nissani N and Leibowitz E 1991 *Int. J. Theor. Phys.* **30** 837
Nissani N and Leibowitz E 1992 *Int. J. Theor. Phys.* **31** 2065
[19] Virbhadra K S 1990 *Phys. Rev.* D **41** 1086
Virbhadra K S 1990 *Phys. Rev.* D **42** 2919